Review Article

Usaid Ahmed Shakil*, Shukur Bin Abu Hassan, Mohd Yazid Yahya, and Mohd Ruzaimi Mat Rejab

A focused review of short electrospun nanofiber preparation techniques for composite reinforcement

https://doi.org/10.1515/ntrev-2022-0116
received August 30, 2021; accepted May 2, 2022

Abstract: Short nanofibers have been of interest in preparing 3D porous structures, aerosol filters, and nanocomposites. These materials require nanofiber retrieval and application in short form with simultaneous control over aspect ratio. Electrospinning, conventionally, offers minimal control over short nanofiber yield as nonwoven mat is the default configuration of collected sample. High surface area to volume ratio nanofiber, however, can offer new vistas in material design if standardization of short nanofiber preparation practices, offering control over aspect ratio, can be attained. It will provide novel insights into design of tissue engineering scaffolds, filtration membranes, and nanocomposite properties. This work summarizes reported efforts to prepare short nanofiber through mechanical, chemical, material, and operational variables. It aims to provide comparative glance at attempts to control aspect ratio along with pros and cons of the adopted techniques. Lastly, discussion shares generalized conclusions and insights gathered while reviewing material and operational variables adopted for short nanofiber preparation.

Keywords: short nanofiber, electrospinning, deformation and fracture, aspect ratio, particles, nanosize

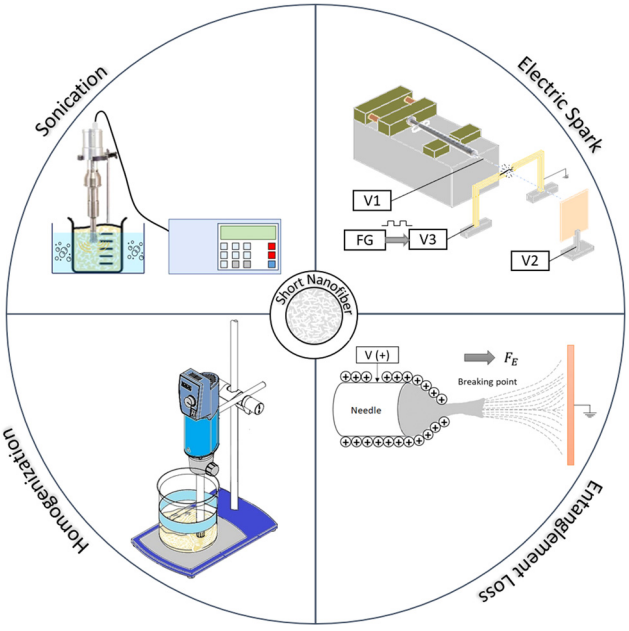

Graphical abstract

1 Introduction

Short or staple fibers are a promising reinforcement for polymer matrix composites [1]. Especially, within the domain of nanocomposites, nano and micro-scale structures are preferred as reinforcements to improve the mechanical properties by mimicking biological models and responses [2–4]. Control of aspect ratio is of key importance here as it can offer improvement in the mechanical, thermal, and optical properties of the materials.

In the recent past, short fibers have been produced adopting extrusion compounding [5], injection molding [6], and interfacial polymerization [7] techniques. Also, conventional vapor-grown technique offers control of length as a function of catalyst activity, process time, and catalyst size [8,9]. Longer processing route and post-processing steps make this approach suitable for

* **Corresponding author: Usaid Ahmed Shakil,** Centre For Advanced Composite Materials (CACM), Universiti Teknologi Malaysia, 81310, Johor Bahru, Malaysia; School of Mechanical Engineering, Universiti Teknologi Malaysia, 81310, Johor Bahru, Malaysia, e-mail: usaid.ahmed98@gmail.com, tel: +60 1117256049
Shukur Bin Abu Hassan, Mohd Yazid Yahya: Centre For Advanced Composite Materials (CACM), Universiti Teknologi Malaysia, 81310, Johor Bahru, Malaysia; School of Mechanical Engineering, Universiti Teknologi Malaysia, 81310, Johor Bahru, Malaysia
Mohd Ruzaimi Mat Rejab: Faculty of Mechanical and Automotive Engineering Technology, Universiti Malaysia Pahang, 26600, Pekan, Malaysia

industrial production. Pressurized gyration combines centrifugal spinning and blowing to produce nanofiber with diameter and length in the range of 60–1,000 and 200–800 mm, respectively [10]. These diverse mechanical, thermal, and polymerization processes have been instrumental in nanofiber fabrication with yield varying in length from nanometers to millimeters. However, there is a trade-off between yield and aspect ratio *i.e.*, techniques that are convenient for mass production offer much higher length whereas those giving nano-meter length do not offer high yield. This is true when we juxtapose post-production and *in situ* production techniques. Where yield of short nanofiber is low, for entanglement loss technique, a greater control over length distribution offers access to desired aspect ratio. This, however, is not the case for post-production techniques, sonication, and mechanical mixing, where a high yield is associated with wider length distribution and hence, a relatively lower degree of control over aspect ratio.

Electrospinning has proved to be a reliable method to fabricate diverse polymeric nanofibers with diameter in nanometers. A polymer solution is, in electrospinning, forced to form cone-jet under the application of electric field. Surface charge on cone induces stretching to elongate the cone thereby producing nanofiber morphology. Electrospun nanofibers have been an attractive option to prepare sensors, filters [11,12], tissue engineering scaffolds [13–15], strategic textiles [16,17], nanocomposites [18], biomedical [19], and healthcare applications [20]. Wider usage of nanofibers is found in material science community although traditional electrospun nanofiber production is limited to mats [21] and sponges [22]. Several techniques have been employed to obtain short nanofibers. Mechanical cutting, by far, has been utilized extensively to prepare short nanofiber suspensions. Electrospun nanofibers, with high surface area and sub-micron diameter, differ in mechanisms that are associated with microfiber breakage or fracture. Highly aligned polymeric chains, intermittent crystalline-amorphous phases, and material properties of individual polymers make scission of nanofiber a complex phenomenon. Additionally, high surface area of nanofiber make short fiber preparation and retrieval difficult because of agglomeration [23,24].

This review offers a focused summary of short nanofiber preparation techniques with mechanisms inducing nanofiber breakage. Techniques employ mechanical, chemical, electrical, and material variables to cut nonwoven mats into short nanofibers with varying degrees of success. The aim is to identify the efficacy of disparate techniques in offering control over aspect ratio and draw conclusion from adopted short nanofiber preparation practices together with commenting on their applicability in composites as reinforcements.

2 Background

Conventional approaches such as compounding and chemical vapor deposition to prepare short nanofibers have history of decades. Their usage in composite industry to reinforce matrices to improve bulk properties is well established. However, complexities ranging from raw materials to process control, on the one hand, and energy intensive fabrication to environmental concerns, on the other hand, have led to a search for reliable, clean, and user-friendly techniques to fabricate nanofibers. Following paragraphs provide an overview of most common techniques of short nanofiber preparation, for composite reinforcement, while simultaneously juxtaposing them with electrospinning.

Compounding through injection molding or extrusion are conventional approaches to fabricate short fiber-reinforced polymeric composites [5,25,26]. The technique involves incorporating microfiber roving in meltable matrix and allowing shear forces to shorten fiber length. Resultant composite properties, here, often depends on the final length of the fibers and volume fraction. Fracture phenomenon, in this case, is an outcome of complex interactions between (i) fiber–polymer (ii) fiber–fiber, and fiber–machine surface. Stress concentration induced by fiber abrasion and flexural stresses resulting from fiber overlap are operational in these interactions. In addition, importance of processing parameters like rate of flow, temperature, and pressure makes the equation much more complex. Also, when factors like nature of resin and fiber volume fraction add to it, process becomes intricate to handle. A higher fiber volume fraction has been reported to offer decrement in fiber length perhaps due to greater fiber–fiber interaction [27,28]. The limitations of the procedure lie in several domains. First, the procedure is suitable for thermoplastic composites only which leaves thermoset out of scope. Second, very high-volume fractions of reinforcements need to be added to improve the properties essentially because the surface area of the fiber is significantly lower compared to the nanofibers. Third, properties of composites are likely to improve in one-dimension as operation of mixing equipment induces directionality of reinforcement in flow direction [6]. This reduces the chances of improving bulk properties. And, lastly, determining nanofiber length demands additional step of pyrolysis to separate nanofiber from matrix after fabrication.

Pyrolysis of hydrocarbons such as natural gas, carbon monoxide, and acetylene can produce carbon nanofibers with length and diameter in the range of 50–100 μm and 50–200 nm, respectively [9]. The technique has been reported to be efficient for mass production of nanofibers at a moderate cost [29].

Decomposition of feedstock enables the fiber growth once suitable features of catalyst are present. Multiple parameters affect the thickness including catalyst activity, operational environment, and size of the catalyst [29]. A major impediment in getting a desired combination of size and length is that the thickening starts once the catalytic activity slows down and temperature rises. Additionally, since filaments clog towards the end of reactor tube, it deposits a thick carbon layer over them thereby producing large clumps. This exterior layer has different properties than more graphitic interior cylinder. Also, heat treatment of nanofibers is imperative since the produced product has disordered graphene plane. Although, heat treatment is reported to increase crystallinity of the nanofiber, it has been associated with decline in electrical and mechanical properties by producing discontinuous crystallites [30]. Therefore, careful optimization of treatment parameters makes the technique demanding and tedious [31]. Lastly, pyrolysis and heat treatment of short nanofibers are energy intensive processes that require skillful supervision and sufficient resources to maintain production facilities.

Electrospinning is a versatile technique to spin nanofibers. In contrast to conventional approaches, production scope of electrospinning covers polymeric [32], ceramic [33], and metallic [34] materials. It offers a freedom to shorten nanofiber both during production and post-production stages. Although, in-production stage requires careful optimization of electrospinning parameters, post-production stage often relies on mechanical or chemical routes independent of spinning parameters. Spinning and solution parameters are important in controlling diameter and morphology of short nanofibers. Viscosity, surface tension, and polymer concentration have been reported to influence diameter [17,35]. In addition, geometrical features can be controlled through machine parameters such as voltage [36], flow rate [37], and tip to collector distance. Similarly, alteration of spinning and solution parameters to spin short nanofibers is well reported. For instance, effect of feed rate [38], voltage [39], and solution concentration [40,41] on *in situ* short nanofiber production reveals the scope of option available to retrieve nanofibers with desired diameter, morphology, aspect ratio, and yield or a combination of these. Post-spinning techniques have an added advantage of preparing nanofiber with features that are conducive in shortening them with suitable solvent. This suspension can be used for bulk modification of matrices or to construct nanostructures for sensors or tissue engineering scaffolds. Keeping in view the much wider control electrospinning offers on short nanofiber production with desired features, it is expected to replace conventional techniques in application areas of nanocomposite, membranes, and biotechnology.

Electrospinning offers nanofiber with diameter in the range of 50–900 nm and fiber can be collected in random mats configuration. Salient features of nanofiber that makes electrospinning a promising choice for fabrication include better mechanical properties, molecular chain alignment, high surface area to volume, and aspect ratio. Size dependent mechanical behavior is evident in nanofibers *i.e.*, improvement in strength, modulus, and toughness *etc.*, with diameter reduction from micro to nano-scale [42]. This effect is coupled with highly crystalline structure of the nanofibers and higher degree of molecular orientation. Several research studies have demonstrated it including one by chew *et al.* [43]. In this study, tensile modulus of nanofiber was altered from 300 to 3,200 MPa and tensile strength from 20 to 200 MPa when diameter reduced from 5 μm to 200–300 nm range for polycaprolactone. Similar results have been obtained for other nanofibers such as polyamide, carbon, and polyimide (PI) nanofibers [44–46]. Size effect phenomenon is augmented by at least three aspects *i.e.*, high molecular orientation induced by electric force, higher concentration of crystalline region, and less core/surface defects per unit area [42,44,47]. Nano dimension of fibers brings aspect ratio (L/D) which is hundreds of times higher than that of the microfibers. Better mechanical performance of continuous fiber composites, partly results from the fact that reinforcement effect is dependent on aspect ratio. Short fiber (low aspect ratio) composites behave poorly because of the following reasons: fiber edges bring stress concentration; fiber agglomeration reduce reinforcing effect; and critical fiber length is indispensable for effective fiber-matrix load transfer. Jiang *et al.* introduced short PI fiber (L/d = 100–200) in PI matrix to compare performance with long fiber interleaves. It was concluded that 2 wt% tensile strength of short fiber composite gave performance equivalent to 38 wt% of long fiber composite [48]. High strain rates and draw ratio induce molecular orientation along fiber axis during electrospinning. Advanced techniques such as transmission electron microscope (TEM), atomic force microscope (AFM), and Raman spectroscopy have been utilized to determine chain alignment in nanofibers [49]. Jiang *et al.* concluded that thinner nanofiber has higher molecular orientation as against thicker nanofiber simply because molecules will have space to randomly locate themselves in higher diameter fiber [50,51]. Carbon nanotubes have diameter around 30 nm and possess specific surface area of 100 m^2/g; on the other hand, human hair diameter is about 60 μm and surface area of 0.05 m^2/g. Typical electrospun nanofibers offers a specific

surface area in the range of 300–3 m^2/g [11]. Higher surface area makes distinct nanofiber characteristics such as high contact area with matrix, improved fiber–matrix adhesion, and better load transfer.

3 Short nanofiber preparation

3.1 Mechanical cutting

Mechanical cutting is a facile approach that offers varying degree of control over nanofiber length and relative effectiveness in retaining morphological features. Xu *et al.* electrospun polyacrylonitrile (PAN) nanofiber to prepare PI composites [52]. Small flakes of nanofibers were ground for 1 h, ultrasonicated (10 min) in ethanol, and dried (60°C) for 4 h. Microscopic characterization revealed short nanofiber length in 3–7 μm range (Figure 1(a)) with aspect ratio between 7.5 and 23.3. Grinding of nanofibers is likely to damage morphology as milling action has been reported to induce flake-like morphology of nanofiber [24], a fact author left unverified. Yoshikawa *et al.* fabricated brush-like symmetry of hydrophilic poly(styrene sodium sulfonate) on electrospun nanofibers of a polystyrene-based hydrophobic copolymer to assess suitability of the solvent system for hydrophobic polymers [53]. Copolymer had reactive sites for surface-initiated atom transfer radical polymerization (SI-ATRP). Mechanical cutting of nonwoven mat, in water and phase-separated systems of water and hexane, using a homogenizer was pursued after 3 h of polymerization. Generally, the fiber length became shorter and more uniform with increment in cutting time. The mean length was 11 ± 17 μm after 3 h of cutting. Homogenization did not affect the morphology or fiber diameter as confirmed from SEM images. Nanofiber cutting facilitated by using a mixture of water and hexane as nanofiber collection at interface of two liquids helped them encounter the blades. However, polystyrene nanofibers without brush-like symmetry escaped the blade action owing to their tendency to float on water surface, hence offering poor dispersion even after long hours of cutting. Overall, nanofiber cutting through homogenizer provides advantages of short processing time, ease of operation, high yield (80%), and control over length (few to tens of microns). This report claimed that length can be controlled through both batch

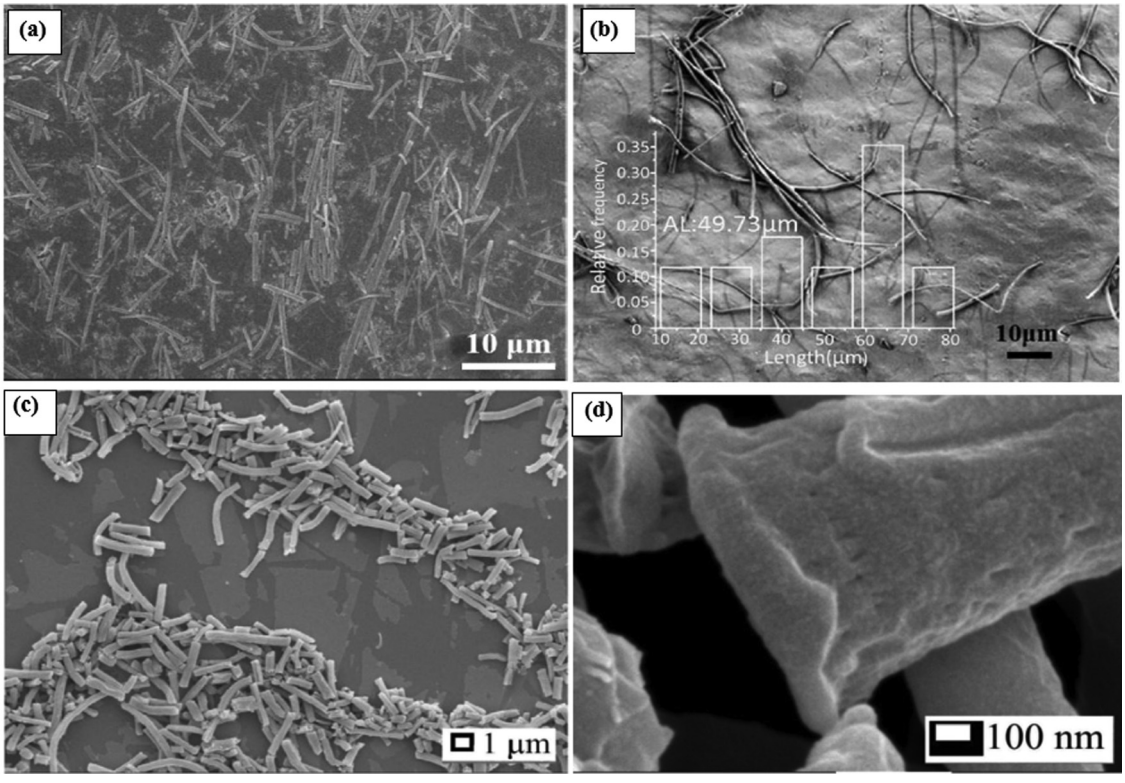

Figure 1: Short nanofiber of (a) brittle PAN with average length range of 3–7 μm [52]; Copyright 2013, reproduced with permission from Elsevier Ltd, (b) composite nanofibers (GO/Iron oxide-reinforced PAN) with average length of 49.73 μm [59]; Copyright 2013, reproduced with permission from Elsevier Ltd, (c) ductile irradiated poly(lactic acid) (PLLA) with average length of 5 μm [24], and (d) pitting of PLLA nanofiber [24]; Copyright 2013, reproduced with permission from Elsevier Ltd.

size and processing time without any attempt to prepare different batch sizes. Huang *et al.* developed nanofiber recipe, with grafted poly(sodium styrene sulfonate) on initiating moiety, with an aim to shorten them and act as cell growth scaffold [54]. A water–hexane mixture was used to disperse nanofibers and homogenization was carried out for 3 h. An average length of 11 ± 17 μm was attained, with higher dispersion, when poly (sodium styrene sulfonate) was grafted as brushes. This behavior was induced by hydrophilicity of the grafted material. Further studies require to investigate the effect of grafted materials content on the fiber cutting efficiency. Kriha *et al.* prepared composite nanofiber by adding cobalt nanoparticles in P(MMA-*c*-VA) polymer solution [55]. The aligned electrospun nanofibers (1–3 μm diameter) were cooled under liquid nitrogen and cut to a length of 50–100 μm, using standard razor blade. Distinctive aspect of the adopted procedure was the retrieval of rod-like non-aggregated short nanofiber. There was no report of fiber length distribution to estimate the efficiency of the cutting procedure. Zhao *et al.* homogenized PI nanofibers to obtain short nanofibers with average length of 300 μm [56,57]. There was no attempt to establish parametric correlation to short nanofiber generation in the reported work.

Deuber and Adlhart reported a facile method of controlling the aspect ratio of water-soluble pullulan/PVA nanofibers [58]. Fiber length of 40 μm and aspect ratio of 140 were achieved after homogenization (13,000 rpm) of PVA nanofiber, in 1,4-dioxane solution, for 20 min. Wetting of nanofiber by the solvent was believed to be crucial to facilitate cutting. Feng *et al.* reported graphene and iron oxide-reinforced composite short nanofiber (d = 300 nm) preparation using homogenizer [59]. Nanofiber pieces of 1 cm × 1 cm were immersed in tert-butanol to agitate under higher shear forces (16,000 rpm) for 40 min. Average nanofiber length was of 49.73 μm (Figure 1(b)). Li *et al.* cut GLA/PVA nanofibers by mixing small fragments in ter-butanol with homogenizer (IKA T-18) operated for 15 min at 13,000 rpm [60]. Short nanofiber length of 27 μm was reported without standard deviation. Silica and PAN mats were cut and dispersed in camphene (100 mL) at 70°C by Si *et al.* [61]. Solution was homogenized for 30 min at 13,000 rpm to retrieve short nanofibers of 50 μm length. There was no report of attempt to measure statistical average diameter of the nanofibers through a range of 100–300 nm. In an identical study, Si *et al.* fabricated aerogels by dispersing silica nanofibers in 200 mL of pure water to homogenize it at 13,000 rpm for 20 min [62]. Short nanofiber length was not reported. Similarly, short PAN nanofibers (decorated with gold) of length 650 ± 218 μm were retrieved by mixing them with dioxane at 5,000 rpm and duration of 35 s [63]. Jiang *et al.* added electrospun PI nanofibers, in small pieces, to solvents (dioxane/water) [64]. After cooling with liquid nitrogen, the resultant paste was cut by operating the mixer at 3,500 rpm for 2 min. Average length was 14 ± 6 μm when the average diameter was 75 nm. Identical methodology was adopted to prepare short PI nanofiber in length distribution range of 20–40 μm [57].

Duan *et al.* irradiated non-woven nanofiber mat for 5 h from 15 cm to cross-link poly(MA-*co*-MMA-*co*-MABP) and PAN [65]. Then, these were mixed with dioxane and cut with razor blade for 45 s at 5,000 rpm. Different weight percentages of nanofibers were used to prepare aerogel although without length characterization. Adopting identical technique, another study from same group reported 150 ± 30 μm short nanofiber length [66]. Blender cutting was utilized to attain short nanofibers of PLA/PCL by mixing them with H_2O/*t*BuOH (500 mL) solvent. Short nanofiber diameter to length ratio of 1/150 μm was obtained [67]. Drummer employed same equipment to prepare short PAN nanofiber in water mixture [68]. Cutting was performed for 10 min at 23,000 rpm to retrieve short nanofiber of length 442 ± 171 μm. A similar work reported 416 ± 83 μm short PAN nanofiber length after nanofiber yarns were mixed with ethanol/water and cut in liquid nitrogen-assisted solidified condition [69]. Short yarns were sonicated to disperse nanofibers. Jiang *et al.* irradiated cross-linkable PNIPAM fibrous mat before mixing them with dioxane and mechanical cutting through mixer for 1 min at 5,000 rpm [70]. Reported short nanofiber length distribution was 100 ± 60 μm.

Xu *et al.* blended cellulose acetate (CA)/ polycaprolactone (PCL) nanofiber mats with deionized water and ethanol. Operation lasted 10 min at 19,600 rpm [71]. A uniform suspension of short nanofibers with length of 95.2 μm was obtained. Since a mixture of CA and PCA was used to spin nanofibers, it would have offered additional insight if the effect of either polymer on the fracture of nanofiber had been explained. Same author treated PAN and PI nanofibers with oxygen-plasma to improve hydrophilicity [72]. Nanofibers were blended in water/ethanol to attain 113 and 133 μm nanofiber length for PAN and PI, respectively. Brittleness of PAN was believed to facilitate mat fragmentation and lower length range. To prove the effect of hydrophilicity in enhancing the cutting efficiency, further investigation requires comparing the results with non-treated nanofiber mats. Another study by the same author combined features of earlier works by blending PAN and PI nanofiber chunks in ethanol [73,74]. Again, blending continued for 10 min at 19,600 rpm. Average length of short nanofibers was reported to be 123 μm though without considering the difference of PAN and PI

nanofibers and their comparison. Using identical materials, equipment, and parameters, nanofiber length from tens to hundreds of micrometer was reported [75]. Cellulose acetate was electrospun and hydrolyzed by the same group to prepare short nanofiber suspension [76]. Blending was done using identical parameters with water as carrying medium. Short nanofibers with average length of 50 ± 15 μm were obtained. Although intact morphology was reported after treatment, author did not comment how treatment can affect nanofiber generation. Zhu *et al.* fabricated poly(bis(benzimidazo)benzophenanthroline-dione) nanofiber for sponge preparation [77,78]. Nanofiber mats were put in electric mixer along with 1,4 dioxane to be stirred 10 times, each time for 30 s. A wide length distribution of 50–500 μm was obtained.

This author's attempts to shorten nanofibers using homogenizer or blender led to clogging of the chunk in drive shaft head of the equipment. This has not been reported in studies using homogenizer except a study by Xu *et al.* [79] where large chunks were used again to prepare nanofibers. This phenomenon limits the technique's application in studies requiring pre-determined nanofiber mass fraction.

Thieme *et al.* synthesized triblock copolymers made up of poly(ethylene oxide) (PEO) and polylactide (PLA) and transformed it into nanofibers by the electrospinning process [7]. Mechanical cutting (motor-driven blade) of liquid nitrogen solidified ethanol (200 mL) and nanofiber (40 mg) suspension was carried out at 26,000 rpm for 10 min. Short Nanofibers were separated by centrifugation at 35,000 rpm. The obtained fiber had a length in the range of 5–15 μm that satisfied the criterion of being below 15 μm, acceptable for inhalation therapy, although length distribution was not reported. As differential scanning calorimetry results confirmed the presence of amorphous PLA and crystalline PEO phases, this can be further investigated to assess effect on nanofiber breakage. Jiang *et al.* produced nylon 6 mat with mean fiber diameter of 163 nm to be cut mechanically into short fibers [80,81]. Nylon 6 dispersion in dimethylformamide was prepared by cutting with rotation blades (RPM: 15000) at −13°C for 5 min. Nanofiber length range of staple nanofibers was few to tens of micron. Langner and Greiner cut poly(acrylic acid) (PAA) nanofiber (2.4 g) in a solution (2-propanol and demineralized water), at −18°C, using a blender for 1 min operating at 3,500 rpm [82]. Short nanofibers with an average length distribution of 87 ± 53 μm were retrieved. Boda *et al.* prepared collagen-gelatin (PCG) nanofiber of average diameter 249 nm [83]. Subsequently, membranes were mineralized (NaCl [1,000 mM], $CaCl_2$ [25 mM], and $NaH_2PO_4{\cdot}2H_2O$ [10 mM] in deionized water). Mineralized nanofibers were, first, frozen at −80°C and then cryo-cut at −20°C. As the diameter increased to 1,758 nm after mineralization, heavy mineral deposition offered aggregates of nanofibers instead of dispersion of individual fibers. Short nanofiber fragments (20 μm) were obtained after freeze drying. Apparently, higher diameter and mineral coating might have facilitated the fracture of fibers. Further studies focusing on changing mineral content and mineralization time will reveal whether agglomeration can be controlled.

Zhang *et al.* aimed to shorten ductile PLA nanofiber (625 ± 278 nm diameter) length, using mechanical stirring and ultrasonication in toluene/petroleum ether (T/P) dispersant media, for composite reinforcement [84]. Sonication was carried out (at amplitude: 40%; Pulse mode: 2 s/2 s) for 2 min. For mechanical cutting, solution was stirred for 24 h at 1,500 rpm using a magnetic stirrer. Short nanofibers could settle as sediment and the supernatant was decanted. Effectiveness of sonication in breaking the ductile polymer nanofibers was minimal. Additionally, yield of short PLA fibers was higher with higher toluene concentration probably owing to partial swelling of PLA in toluene. The surface of nanofibers became rougher and pitted, without fracture, at low volume fraction of toluene (T/P = 30/70). At higher concentration (T/P = 80/20), morphology change was noticed. To correlate toluene concentration (10–100% toluene in petroleum ether) with ease in fragmentation, mechanical stirring method was adopted. At a toluene concentration approaching 80%, stirring produced fiber with lengths of 50–700 μm range. The average length of the PLLA fibers was 220 ± 112 μm with most of the cut fibers' lengths lying in 100–200 μm range. Since toluene concentration of 80% produced damaged and intact morphology during sonication and stirring, respectively, effect of temperature rise, during sonication, on morphology needs to be carefully sorted out. Chen *et al.* received different weight fraction of gelatin/PLA nanofiber ($1\,cm^2 \times 1\,cm^2$) membranes in ter-butanol solvent to prepare short nanofibers for 3D-scaffolding [85–88]. The mixture was homogenized for 15 min at 12,000 rpm. At least 50 random measurements of nanofiber length were taken using optical microscope. Average fiber length and diameter were 86 μm and 1,114 nm, respectively, although nanofiber length range was 4–600 μm. Adopting same nanofiber material, nanofiber homogenization fractured brittle gelatin into groove fibers of 14.6 μm length [89]. Similarly, Deuber *et al.* electrospun pullulan/poly(vinyl alcohol) nanofibers (d_{avg} = 240 nm) to be used in aerogel preparation [90]. Nanofiber mat pieces ($1\,cm^2 \times 1\,cm^2$) were dispersed in 1,4-dioxane and homogenized (IKA T25) for 20 min at 13,000 rpm. Fiber length distribution of 48.8 ± 30 μm was obtained. Duan *et al.* electrospun poly(2VP-*co*-MABP), poly(MA-MMA-MABP), and PAN

nanofibers and did curing using UV light [63]. Gold nanoparticles were anchored on mats after improving their hydrophilicity through ammonia treatment. Short nanofibers in dioxane were retrieved using rotating mixer operated at 5,000 rpm for 35 s. Average fiber length of 650 ± 218 μm was used to fabricate sponges using freeze drying method. Si *et al.* homogenized PAN and silica nanofiber in camphene at 70°C [61]. Homogenization time and rpm were 30 min and 13,000, respectively. Uniform nanofiber dispersion with an average length of 50 μm was attained. Another study utilized pre-oxidized electrospun PAN nanofiber to retrieve short nanofibers with length in the range of 40–60 μm [91]. For that, nanofiber piece was homogenized in water/ethanol mixture at 13,000 rpm for 30 min.

Xu *et al.* utilized blending operation to retrieve short nanofibers of PAN and PI [73]. First, nanofibers were treated with oxygen plasma, to make the surface hydrophilic, and then cut into 1 cm × 1 cm pieces to be immersed in deionized water. The suspension was blended for 10 min at 19,600 rpm to get nanofibers with an average length of 123 μm. Another related route employing mechanical/physical force was reported by Deniz *et al.* [92]. Titanium nanoparticle solution with polyvinylpyrrolidone was prepared and electrospun to get bead-free nanofibers (d_{avg} = 200 nm). These nanofibers underwent calcination to attain pure titania nanofibers. Mortar and pestle-assisted crushing of the nanofibers produced nanofibers in 1–10 μm range. Crystalline structure of the nanofibers was confirmed through XRD, and the brittleness was believed to facilitate fracture of the nanofibers in such a short length range. These short nanofibers were successfully dispersed in thermoplastic polymers to electrospun composite nanofibers. Despite setting the scope of preparing short titania nanofiber with different polymers, no correlation between nature (soft/rigid) of polymer and ease/shortening of nanofiber was drawn. Yao *et al.* spun PCL/PLA nanofiber and cut them into flakes to be mixed with ethanol [74,93,94]. Soaked pieces were solidified using liquid nitrogen and ground using mortar and pestle. The product was sieved through 1 mm mesh to sift larger pieces and to be returned for grinding. There was no attempt to measure the length of short nanofibers.

In addition to the works summarized above, there has been attempts to prepare short nanofibers from homogenization, primarily, and through other mixing methods but without reporting or measuring nanofiber length [62,65,74,93,95–98]. This might have been owing to insignificance of length characterization for the application intended.

3.2 Ultrasonication

Mechanism of sonication involves bubble generation in fluid that grows and collapses thereby releasing energy. Bubble growth, initiating at cavities, can be up to 50 mm in diameter under negative pressure [99]. Time order of bubble generation and collapse are in μs and ns, respectively [100]. This method has been effective for the cutting of carbon nanotubes [101]. Sawawi *et al.* conducted study on several nanofibers using mechanical- and ultrasonic-assisted arrangements [24]. Sonication was carried out using a sonicator (power: 750 W; probe dia: 13 mm) working at 20 kHz. Pulse mode of 2 s/2 s and amplitude of 80% were adopted and experiments were conducted in a sonication time of 1–35 min. Short nanofibers of poly (methyl methacrylate) (PMMA) and polystyrene (PS) were detected after sonication time of 40 and 60 s, respectively. Measured lengths were 10.3 ± 5.6 and 10.5 ± 6.2 μm for PMMA and PS, respectively. Whitish color of the supernatant indicated a degree of homogeneity achieved and scission of nanofibers. Distinctive aspect of the study was breakage of the ductile fibers such as PLLA as brittle PAN nanofiber fracture was possible through sonication alone. Realizing the higher ductility of these nanofibers through tensile tests, PLLA membrane was irradiated for 12 min with the intensity of 14.75 mW/cm^2 by UV Ozone Procleaner prior to sonication. PLLA short nanofiber with length in the range of 5 ± 5 μm were obtained (Figure 1(c)) with localized fiber etching evident in SEM images (Figure 1(d)). It seemed that the micro jetting and erosion created rougher weaker zones. Further investigation on PS nanofibers revealed that average fiber length (6 ± 2 μm) of random nanofibers was higher than that of aligned nanofibers (3 ± 1 μm). Also, aligned nanofiber sonication at temperatures of 30 and 90°C showed no significant effect on nanofiber lengths. This work utilized turbidity measurements to assess degree of nanofiber shortening which might be erroneous as erosion of material from surface, as reported, might change the solution color.

Liu *et al.* tested morphological durability of the SiO_2 (~10 mg) nanofibers by having trace amount of nanofiber placed in a 20 mL glass vial with 10 mL EtOH [102]. The suspension was then subjected to vigorous ultrasonic vibrations (200 W) for three cycles, each lasting 5 min. An important finding was to correlate morphology of the nanofibers with pyrolyzing temperatures (600, 800, 1,000, 1,200, and 1,400°C). In 600–1,000°C temperature window, fiber morphology was retained, and the average aspect ratio of the broken nanofibers was larger than 100. However, above 1,000°C, short fiber bundles were witnessed because of fusion and melting caused at cross

over points of the nanofiber mats. Additionally, it can be concluded that the fiber fracture for brittle materials such as silica is possible although fusing phenomenon induce greater fiber–fiber interaction. Chen *et al.* prepared 5 wt% glass nanofiber suspension in water to be subjected to vigorous ultrasonication using an ultrasonic probe (100 W) [103]. Short nanofibers with few to tens of micrometers in length were obtained. Proper characterization of nanofiber length and distribution was missing. Wang *et al.* sonicated titania nanofibers for 1 h in a mixture of water to attain short nanofiber of 3 μm length [104].

Similarly, Mulky *et al.* conducted comprehensive experiments to investigate the effect of sonication time, temperature, and nanoparticle addition on staple PLLA nanofiber length (Figure 2) [105]. Nanofiber flakes (0.5 cm × 1 cm) immersed in relevant dispersant media were sonicated (400 W, pulse on/off 2 s/2 s). Ice bath was arranged to (ice/acetone) maintain −80°C temperature. Titanium nanoparticle and fiber ratio was 1:1. Average diameter of the electrospun nanofiber was 244 nm and the dispersant media were water, water/ethanol (4:1), and hexane. Key factor was interaction between PLLA nanofiber and dispersant media: surface energy and hydrophilic/hydrophobic character. Water, water/ethanol, and hexane suspensions offered lumps, disintegration of non-woven mat, and disentanglement/fracture of nanofibers, respectively. In water-based suspensions, fiber–fiber interaction was believed to be stronger than water–nanofiber interaction. On the other hand, low vapor pressure of hexane was conducive to cavitation resulting in higher degree of implosion to cut nanofibers. For hydrophilic and hydrophobic TiO_2 nanoparticles, average staple fiber lengths were 63 and 51 μm, respectively, whereas this value for neat nanofiber was 39 μm. As the scope of the study involved investigating the effect of solvent and nanoparticle addition on short nanofiber preparation, there were different outcomes from both the approaches. A hexane dispersion provided complete fragmentation whereas nanofiber agglomerates were excluded from nanoparticle suspension to take length measurement. That makes the nanoparticle addition inefficient route to prepare predetermined mass fraction featured samples. Effect of temperature was investigated, at 0 and −80°C, in hexane. At −80°C, average lengths obtained were 77, 63, 44, and 35 μm after 10, 20, 30, and 60 min of sonication, respectively. At 0°C, nanofiber lengths were 54 and 47 μm in ice bath and ice-acetone bath, respectively. Additionally, it was concluded that below a threshold aspect ratio, induced stresses in nanofiber may not be high enough to fracture them.

3.3 Electrical spark

Basic idea of this technique is to interrupt the electrospinning jet through electric spark periodically to induce thermal energy that will cut the nanofiber. Fathona and Yabuki utilized electric spark to interrupt electrospinning jet to produce short nanofibers (Figure 3(b)) [106]. Aluminum electrodes were placed just next to needle to apply square wave voltage, (f: 30 Hz; duty cycle: 90%), to generate electric spark. The fibers that flew through electrode gap were shortened whereas those evading electrode gap were collected as continuous fibers. The length of the short fiber was approximately 100 μm with one edge curled although a length range of 22–400 μm was recorded in a full experiment. Yield was reported by counting the number of fibers in a unit area. This value was 1–5 short nanofibers per 0.12 mm × 0.2 mm area. Due

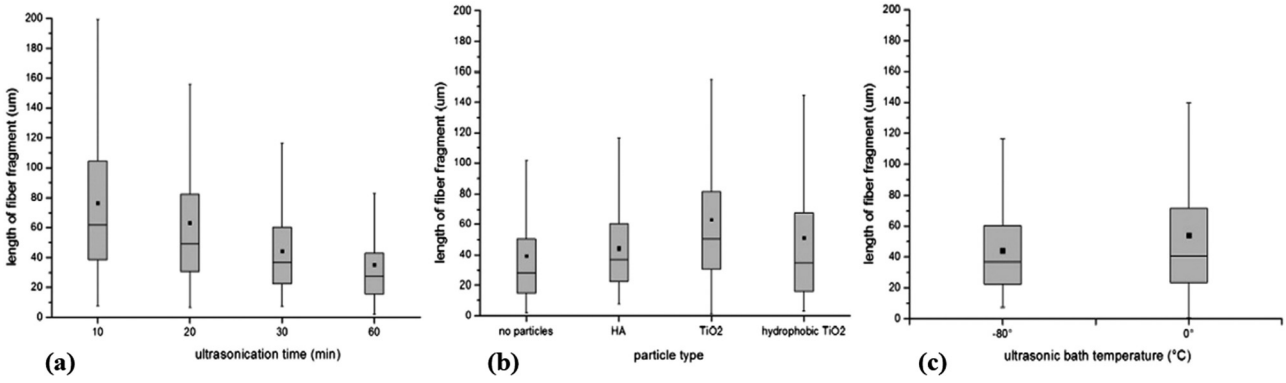

Figure 2: Fiber length distribution in relation to (a) sonication time and (b) nanoparticle type and (c) sonication bath temperature [105]; Copyright 2014, reproduced with permission from Elsevier Ltd.

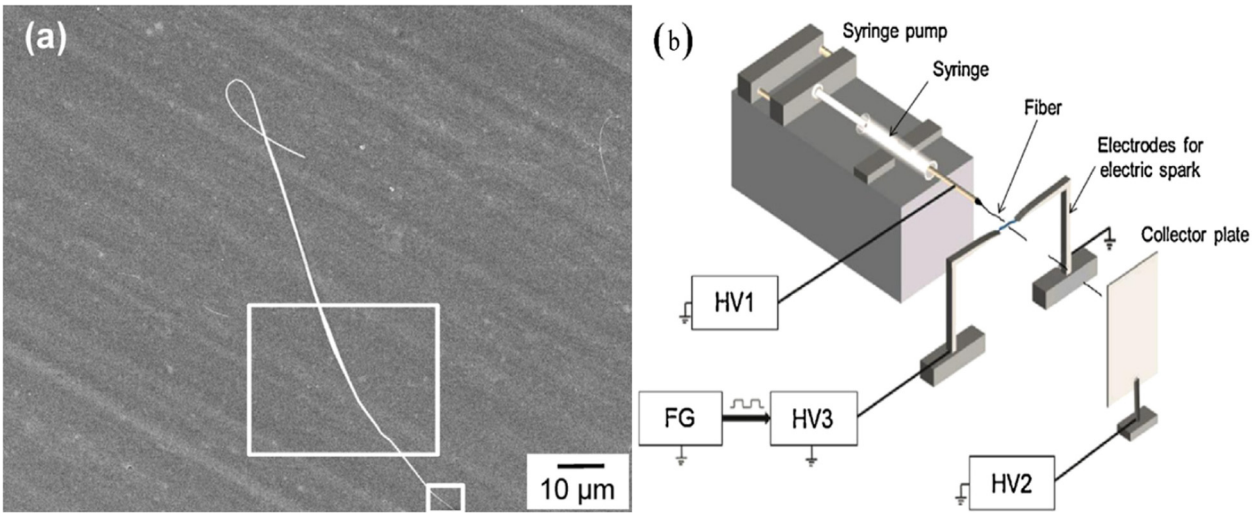

Figure 3: (a) Short nanofiber and (b) schematic of the electric spark mechanism utilized for obtaining short nanofiber [18]; Copyright 2013, reproduced with permission from Elsevier Ltd.

to the limited spark-controlled area (1.5 mm × 0.5 mm), yield of continuous nanofibers was much higher. It was obvious that through periodic activation of electrical field and thermal energy from the spark, electrospun nanofiber was stretched and cut, respectively (Figure 3(a)). Diameter of short nanofiber at edges was smaller compared to diameter measured at center owing to compressive force exerted by the electric field. Spark-activated cutting was demonstrated to be a function of polymer solution velocity, solution jet trajectory, and frequency of spark activation. More studies are required to explore whether flow rate, frequency of spark, and trajectory can help enhance yield and narrow length distribution of short nanofibers.

3.4 Entanglement loss

Solution entanglement number is a fundamental concept considered when selecting polymer–solvent combination. It is a measure of minimum amount of polymer chains, in entangled form, that are necessary to make a continuous polymer jet traveling in electrostatic field. Fathona and Yabuki exploited the idea of altering solution dynamics under electrostatic forces, by changing polymer concentration, to prepare short nanofiber [39]. Acetone/dimethylacetamide (DMAc) (solvent) and cellulose acetate (polymer) were used to prepare dope solution. By lowering polymer concentration below the threshold value required for continuous spinning, short fibers, spun at 13 wt% concentration, with length in the range of 50–150 μm were obtained. However, polymer concentration ranges of 9–12 and 16–18 wt% produced beaded and continuous fibers, respectively. Although it was concluded that the polymer concentration was the most important factor in shortening nanofibers, it missed to relate that fiber length distribution increased with polymer concentration within the concentration window offering short nanofibers. Tungprapa *et al.* reported that 2:1 volume ratio of acetone/DMAc has a low surface tension that had bearing on solvent–polymer interaction [40]. That would alter the tensile strength of the polymer solution to achieve facile segmentation. The average length of nanofiber at 13, 14, and 15 wt% were 130, 180, and 230 μm, respectively. It was expected that the increment in solution viscosity may stretch the jet for a longer distance before breaking. Additionally, fiber length distribution narrowed down when the polymer concentration dropped from 15 to 13 wt%. Once optimum polymer concentration, 13 wt%, was determined, effect of flow rate and voltage was investigated. A flow rate of 0.02, 0.04, and 0.4 μL/min offered average lengths of 65, 120, and 150 μm, respectively, at a voltage of 5.5 kV. Above 0.5 μL/min, continuous fibers were retrieved. When the voltage values were 4.5, 4.7, 5.5, and 7 kV, average fiber lengths were 670, 250, 170, and 40 μm, respectively. An interplay of the following factors led to the formation of short nanofibers: (1) tensile strength of the polymer solution, (2) the lateral perturbation of the surface charge on solution, and (3) longitudinal force. Another insightful study by the same group incorporated titania nanoparticle in cellulose acetate (13 wt%) solution to prepare short nanofibers [107]. Objective was to investigate how nanoparticle surface charge and concentration affect composite nanofiber length. Concentration was 0.5–17 wt% in polymer solution that

translated into 4–56 wt% after solvent evaporation. For analysis, 0, 4, and 38 wt% nanoparticle concentrations were considered representative of concentration range adopted with appreciation of change in length after addition of every 5 wt% of nanoparticle. Diameters range for 0, 4, and 38 wt% nanofibers were 110–150, 250–270, and 310–370 nm, respectively. Average lengths for same concentrations were 120, 112, and 47 μm as shown in Figure 4(a)–(c), respectively. Apparently, nanoparticle addition increased viscosity of the solution thus avoiding jet interruption and breakage to produce nanofibers, the reason why wider length distribution was offered at lower concentration.

An increment of repulsive force, F_R, induced thinning of polymer jet and eventual break (Figure 5). At low concentrations and pH = 4, repulsive force was generated by agglomerates of positively charged nanoparticle and negatively charged polymer thereby stretching the jet (Figure 5(a)). However, at pH = 9, polymer was repelled by negatively charged nanoparticles thus improving dispersion and reducing chances of jet breakage (Figure 5(a)). At higher nanoparticle concentration, either positively or negatively charged agglomerates will induce breakage.

In an another study, Fathona *et al.* altered the inner diameter of electrospinning needle to control nanofiber length [38]. Initial experiments confirmed that the 4.5 kV voltage and flow rate of 0.1 μL/min were conducive to short nanofiber generation. It was reported that nanofiber diameter increased with increment in needle diameter. And for 0.26, 0.16, and 0.11 mm needle diameter, average nanofiber lengths were 123, 80, and 50 μm, respectively. An imbalance of forces of surface tension, coulomb attraction, and net cohesive force of polymer led to the breakage of nanofibers. Thinning and stretching of nanofiber edges was caused by longitudinal force exerted by electric field. An ancillary study can investigate the effect of these parameters on the yield of short nanofiber by counting them per unit area.

Greenfeld and Zussman conducted 76 experiments on PMMA nanofiber to understand entanglement loss relation to short nanofiber production [41]. Electric field intensity and polymer concentration were used as free variables. The polymer concentration "c" was identified with semi-dilute entangled regime with a relative concentration c/c_e (c_e is the entanglement concentration) lying between 1 and 2. This range denotes transition between beads and continuous nanofiber production. In a fluid jet, electrostatic force applied on charged ionic species of solution generates stress. The stress in the jet is directly proportional to $s{\cdot}E$, where E is the electrostatic field intensity, and "s" is the surface charge density. If the stress exceeds the jet tensile strength, the jet will break at weak points. As the effect of the break is no longer significant on the stresses in the jet, the next segmentation occurs at a distance from the previous break point. This mechanism will generate a short nanofiber. Evolution of this phenomenon is shown in Figure 6. In general, the fragment length gets shorter with: (1) increase in the electric field intensity, (2) decrease in the polymer concentration, and (3) decrease in the flow rate.

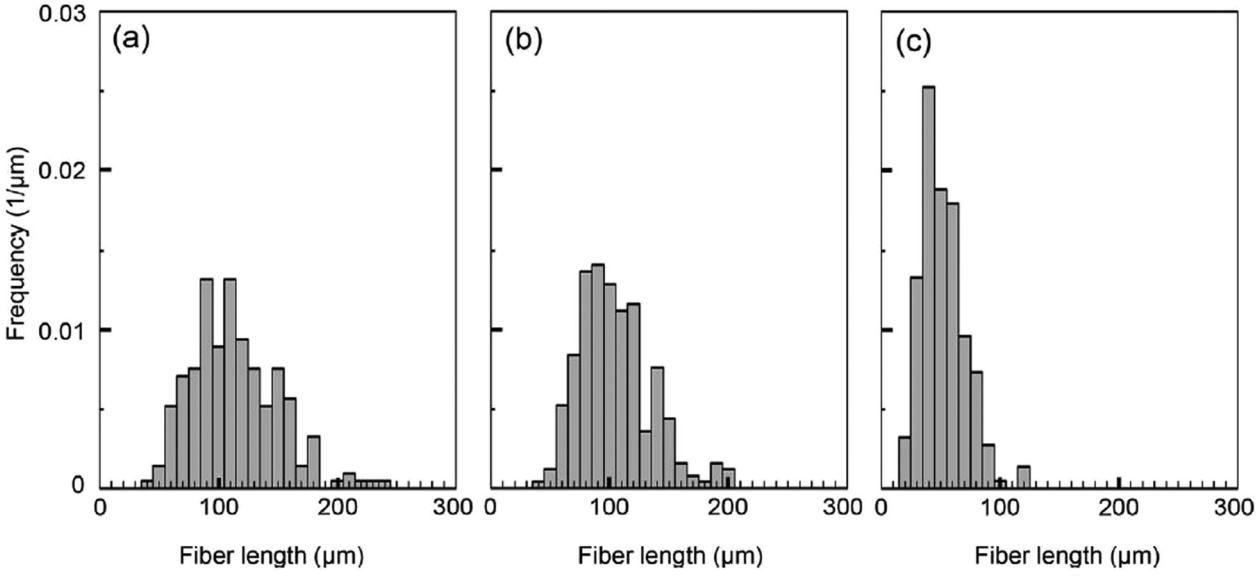

Figure 4: Fiber length distribution of (a) 0, (b) 4, and (c) 38 wt% TiO_2 nanoparticles-reinforced nanofibers [107]; Copyright 2014, reproduced with permission from Elsevier Ltd.

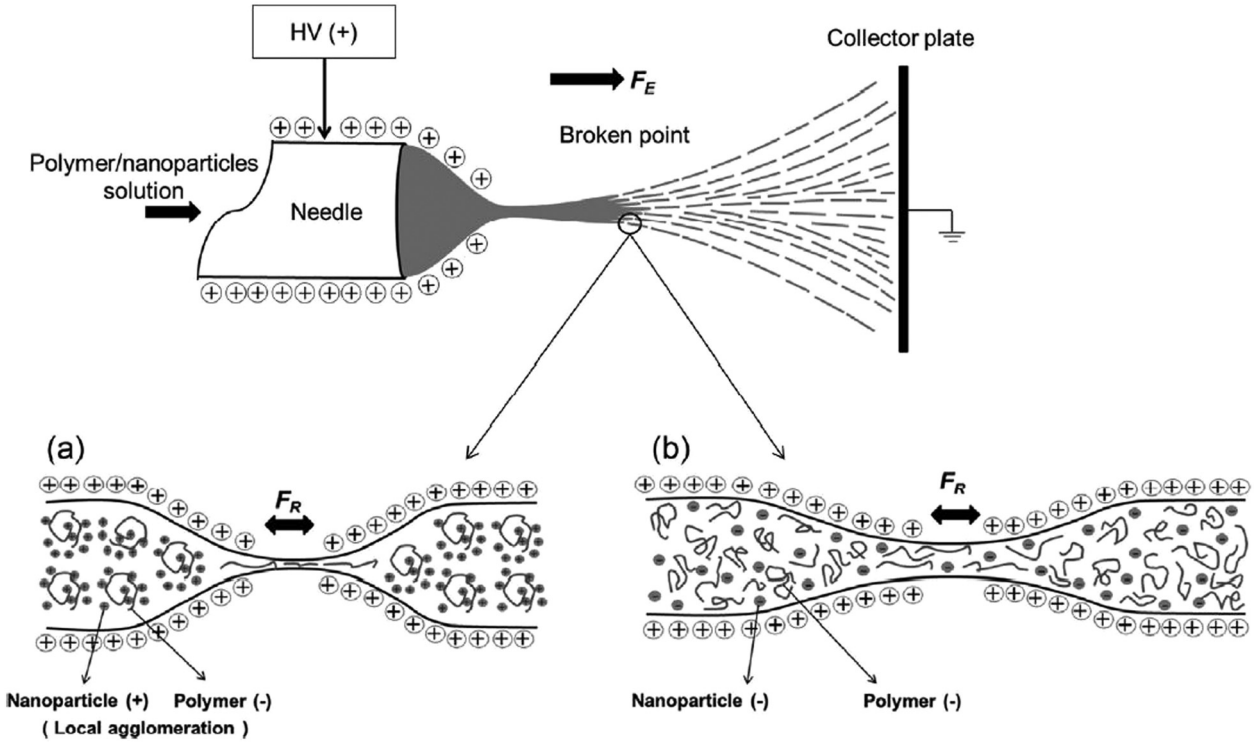

Figure 5: Breakage mechanism and repulsive force generation in polymer jet at (a) pH = 4 and (b) pH = 9 [107]; Copyright 2014, reproduced with permission from Elsevier Ltd.

PMMA nanofiber ranging from 1 to 1,000 μm in length and diameters ranging from 50 nm to 3 μm were collected. More studies are required to confirm the reliability of the technique and whether entanglement loss is possible for both high and low molecular weight polymers, since the solution entanglement number is directly related to number average molecular weight of the polymer [108].

3.5 Chemical treatment

This method, primarily, considers chemical composition (crystalline-amorphous phases) of polymer to exploit it for short fiber preparation. Kim and Park did aminolysis of PLA for 1, 3, and 5 h to retrieve the short form of nanofibers [23]. For aminolysis, a 10 wt% of PLA nanofiber

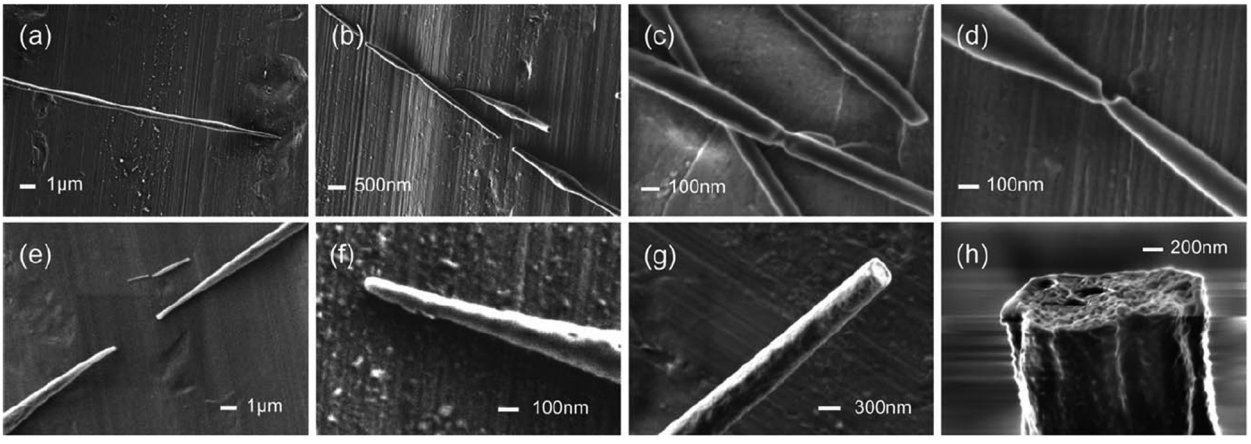

Figure 6: (a) Diameter variation; (b) fragment; (c) neck production; (d) breaking; (e) individual fragments; (f) round end; (g) fractured face; and (h) fractured cross-section [41]; Copyright 2013, reproduced with permission from John Wiley and Sons.

suspension (distilled 1,6-hexanediamine (Aldrich)/2-propanol) was prepared and allowed to react at 37°C. Application of gentle shear stress (orbital shaker: 500 rpm) fragmentated the nanofiber into nanocylinders that were centrifuged and washed, subsequently. Aminolysis degraded amorphous region of the nanofibers and helped in concomitant lamellar crystallization thereby producing semi-crystalline nanocylinders (Figure 7). An increase in aminolysis time (1–5 h) improved fragmentation with mean length decreasing from 15.8 to 5.2 μm; corresponding aspect ratio varied from 48.6 to 16.0. Treatment for an hour was reported to induce dents and cracks on surface but prolonged treatment for up to 5 h was associated with morphology loss. To investigate the effect of fiber diameter on treatment induced nanofiber length, nanofibers of diameter 958, 325, and 152 nm were fabricated and treated for 3 h. Corresponding lengths and aspect ratio were reported to be 5.1, 7.7, and 11.4 μm and 75, 23.7, and 5.3, respectively. Apparently, with diameter reduction, an easy fragmentation was achieved when all other parameters were constant. This might hint at offering higher yield if the total mass fraction of the nanofiber is controlled by keeping diameter low, a relation which requires further investigations to be established.

Celebioglu and Uyar reported successful spinning of γ-cyclodextrin/PEO nanofibers from homogeneous solutions [109]. PEO was chosen as sacrificial matrix to obtain short nanofibers that were believed to enhance volatile organic compound removal. γ-cyclodextrin concentration was kept at 20% by weight but the PEO concentration was changed from 1 to 3 wt%. Non-beaded nanofibers were obtained at all concentrations except 1 wt% PEO. Diameter of the nanofibers increased with the increment in PEO concentration. Chloroform rinsing was conducted for 3 h to dissolve PEO matrix and retrieve short nanofibers. Nanofiber generation was explained by breaking down of long PEO polymeric chains. Author did not report the average length or aspect ratio.

3.6 UV irradiation

Selective crosslinking is another tailorable method to exploit heterogenous composition of nanofiber for short fiber preparation. Stoiljkovic and Agarwal shortened poly (butadiene) nanofiber utilizing ultraviolet irradiation [110]. Two types of masks were used: (1) mask with slit span between 100 and 150 μm and (2) glass plate having narrow palladium strips of 50 μm. Distance between two consecutive palladium strips was 20 μm that determined length of the cut fibers. A UV photoreactor was used to irradiate nanofiber thereby inducing crosslinking. Removal of non-cross-linked polymer was achieved by immersing substrates in suitable solvent for 60–120 s. Nanofiber length range was 100–150 μm in case of random fibers, in correlation with slit span. The length of the aligned fibers covered with 100 μm mask was in the range of 100–160 μm (140 ± 30 μm), whereas the fibers covered with 20 μm mask had length from 20–40 μm (35 ± 5 μm). Microscopy confirmed that fiber cannot be prevented from swelling during solvent treatment. Further studies are required to correlate morphology of the nanofiber with UV exposure time and nature of solvent used for removal of non-cross-linked sections. Basic requirements for this technique were that polymer should be (1) photo-cross linkable and (2) amenable for electrospinning.

4 Comparison of short nanofiber preparation techniques

A review of the published literature reveals that efforts to shorten electrospun nanofibers can be classified in two categories. First is *in situ* production of short nanofibers that relies primarily on changing solution and spinning variables. Second is post-spinning techniques that

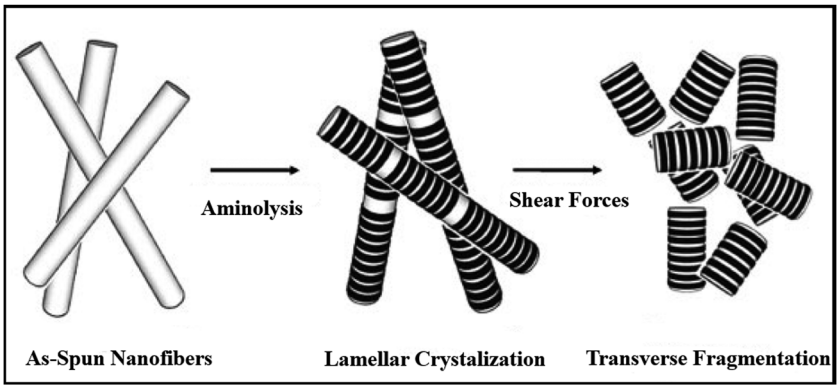

Figure 7: Aminolysis-induced fragmentation and crystallization of PLA nanofibers [23]; Copyright 2018, reproduced with permission from John Wiley and Sons.

utilizes chemical treatment or mechanical forces to fracture nanofibers. A few attempts, involving diameter change, try to correlate solution parameters to ease of nanofiber shortening in post-production stage. However, there has been a general disregard for solution and spinning parameters among those who attempted to shorten nanofibers in post-spinning stages. In this domain, primary focus has been on selecting suitable solvent and sonication/homogenizing parameters together with the choice of polymer (soft/rigid). An overview of these techniques enables now to compare them in terms of basic requirements, pros and cons, and the quality of product they offer.

Mechanical cutting method involves both sonication and high-speed shear mixing with grinding in some cases. The basic equipment for mechanical force-assisted fracturing of nanofibers are advanced high-power tip ultrasonicator and homogenizer. Sonicator and homogenizer, according to literature, with capacity more than 400 W and 10,000 rpm, respectively, are suitable for the operation. Since the nanofibers are processed in a solvent, shortened nanofiber agglomerates and sedimentation are chronically reported issues [83]. Also, as the techniques rely on high power instrument, heat generation is another issue that is countered by an additional arrangement of ice-bath especially in case of sonication. This is particularly true of ductile nanofibers as their structures relaxed with rising temperature thus making fracture phenomenon unlikely to happen [24]. Lastly, a wider length distribution of short nanofibers is offered for both sonication and mechanical mixing. Advantages include immunity from dents or morphology loss of short nanofibers in case of mechanical mixing [53]. Surface roughness and pitting, however, is common for sonicated nanofibers. A correlation between mixing time and nanofiber length exists, in both cases, that offers a degree of control over aspect ratio. Most of the studies report processing time of less than 30 min, relatively shorter duration compared to chemical treatment or entanglement loss. Lastly, higher yield is possible with little consideration of spinning parameters. A special case is of composite nanofibers where nanoparticle concentration needs to be optimized if shortening is achieved through altering spinning or solution variables. This complexity, however, does not exist for mechanical cutting method. Table 1 qualitatively compares the post-spinning techniques in terms of product quality and efficiency.

Treatment of nanofibers can be through chemicals or irradiation. The primary focus, here, is to exploit the physical structure of nanofibers to facilitate scission. The preconditions for irradiation and chemical treatment are photo-cross linkable polymer and presence of amorphous phase, respectively. UV irradiation has been reported to offer precise length control because the sample is exposed to radiation at pre-determined points [110]. On the other hand, chemical treatment times correlate with nanofiber length hence the degree of control is relative [23]. These treatments are often accompanied by morphology loss or swelling of nanofibers as they involve degradation of polymeric structures.

In situ techniques include electric spark- and entanglement loss-assisted nanofiber breakage. The primary difference, between the two, is installation of spark generation setup and alteration of solution and spinning dynamic. Electric spark technique offers very low yield and greater control. Also, morphology damage is obvious as the spark induced heat breaks the nanofiber. Entanglement loss involves manipulating fundamental mechanism of Taylor cone generation and the variables associated with it [41]. Voltage, flow rate, needle diameter, solution concentration, and nanoparticle addition has been exploited so far successfully to spin short nanofibers. Although a continuous process, this technique offers moderate yield. Additionally, extensive iteration is required to optimize the parameters which explains a moderate control over the nanofiber length. It is important to realize that any attempt to control length using solution or spinning variables will affect the

Table 1: Comparison of post-spinning short nanofiber techniques

	Post-production techniques			
Features	**Mechanical cutting**	**Sonication**	**Chemical treatment**	**UV irradiation**
Morphology loss	No	Yes	Yes	Yes
Agglomeration	Yes	Yes	No	No
Correlation of processing time and length	Yes	Yes	Yes	No
Length distribution	Wide	Wide	Wide	Narrow
Yield	High	High	Moderate	Low
Solvent	Yes	Yes	Yes	Yes
Temperature control	No	Yes	No	No
Processing time	Short	Short	Long	Short
Dependence on polymer/spinning variables	Low	Low	High	High

Table 2: Comparison of *in situ* short nanofiber preparation techniques

In situ techniques						
Technique	**Morphology loss**	**Agglomeration**	**Length distribution**	**Yield**	**Processing time**	**Dependence on polymer/ spinning variables**
Electric spark	Yes	No	Wide	Low	Long	Low
Entanglement loss	No	No	Narrow	Moderate	Long	High

nanofiber geometrical features (roughness or diameter). Despite all the complications, there is clear advantage of attaining intact morphology with a narrow length distribution [40]. Also, there is a wide window of variables that can be useful in short nanofiber generation. Table 2 provides a performance comparison of *in situ* short nanofiber production techniques.

5 Potential applications of short nanofibers in composites

For polymer matrix composite reinforcement, short nanofibers can be incorporated with a view to improve bulk or interphase properties. There might be three major routes to incorporate short nanofibers into composites *i.e.*, bulk matrix modification, direct spinning on prepreg, and spray deposition. These applications too have correlation with short nanofiber preparation techniques. For instance, *in situ* fabrication techniques (electric spark and entanglement loss) are suitable for direct spinning on prepreg to fabricate fiber-reinforced nanocomposites. However, post-spinning techniques are conducive for spray deposition and bulk matrix modification. Table 3 summarizes the suitability of short nanofiber preparation techniques with application in composites.

5.1 Bulk matrix modification

Short nanofiber preparation techniques such as mechanical cutting and sonication do involve solvent to facilitate shortening. Selection of a suitable solvent makes them compatible with principles of solvent casting method for nanocomposite fabrication [48]. Here solvent is likely to serve dual purpose as facilitating medium for nanofiber fracture and dispersant. Such a dispersion will be mixed, eventually, with matrix for bulk matrix modification (Figure 9(a)) and solvent will be evaporated using vacuum oven or rotary evaporator. Since homogenization and sonication are conventional mixing techniques for nanocomposite preparation, matrix modification using short nanofibers will incur no additional cost in terms of equipment and materials.

Nature of electrospun nanofiber polymer is another aspect that makes this approach promising. Rigid materials such as PAN [52] and silica [103] are easy to be fractured and collected in powder form for them to be directly mixed in resin. However, heat treatment of these high strength nanofibers and surface treatment such as plasma etching might be associated with surface defects and remaining structural defects, respectively [111,112]. These defects are likely to initiate fracture of short nanoparticles during shear mixing or sonication [113,114]. Shortening of reinforcement will reduce aspect ratio below the critical value required for efficient stress transfer. Such complications with brittle materials might be responsible for degradation of composite properties.

Shortening, however, is difficult to practice in case of soft polymers such as nylon nanofibers. Solvent-assisted dispersion and casting help tackle short nanofibers of soft polymers to improve bulk matrix properties. In addition to nanofiber-reinforced matrix composites, such a recipe can be conveniently adopted to prepare laminates with modified matrix, also called fiber-reinforced nanocomposites, through vacuum bagging.

Table 3: Application of short nanofiber preparation techniques in composite reinforcement

Applications	**Mechanical cutting**	**Sonication**	**Electric spark**	**Entanglement loss**	**Chemical treatment**	**UV irradiation**
Bulk matrix modification	✓	✓	✗	✗	✗	✗
Spray deposition	✓	✓	✗	✗	✗	✗
Direct spinning	✗	✗	✓	✓	✗	✗

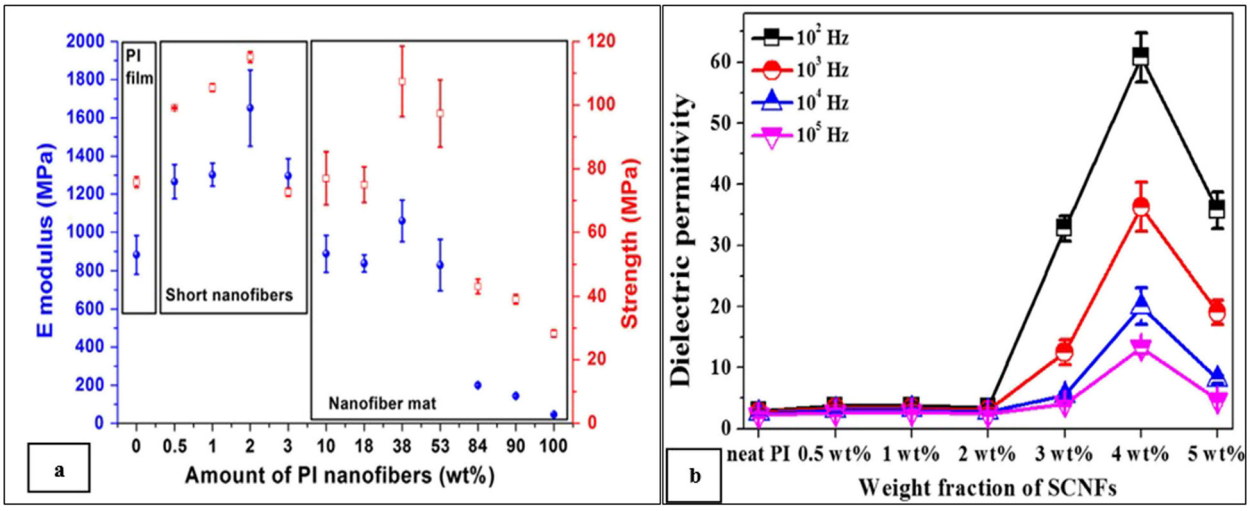

Figure 8: (a) Mechanical reinforcing potential of short nanofiber [48] and (b) improvement in dielectric properties at optimum short nanofiber concentration [52]; Reproduced with permission from Elsevier Ltd.

Other techniques such as UV irradiation and chemical treatment are reported to incur nanofiber morphology loss and alteration in phase structures. This entails poor mechanical properties, hence making them unsuitable for composite reinforcements.

Short nanofibers for bulk matrix modification has been successfully utilized to improve mechanical properties [48,115]. It was concluded that 2 wt% of short nanofiber was as efficient as 38 wt% continuous nanofibers in improving modulus (Figure 8(a)). Adopting similar approach, dielectric properties of PI matrix were improved at an optimum concentration (Figure 8(b)) [52]. Short nanofiber reinforcement has been effective too in improving thermo-mechanical properties of polymer matrix composites and in tailoring interphase responses [116]. There are reports demonstrating the effectiveness of these reinforcement in introducing ductile

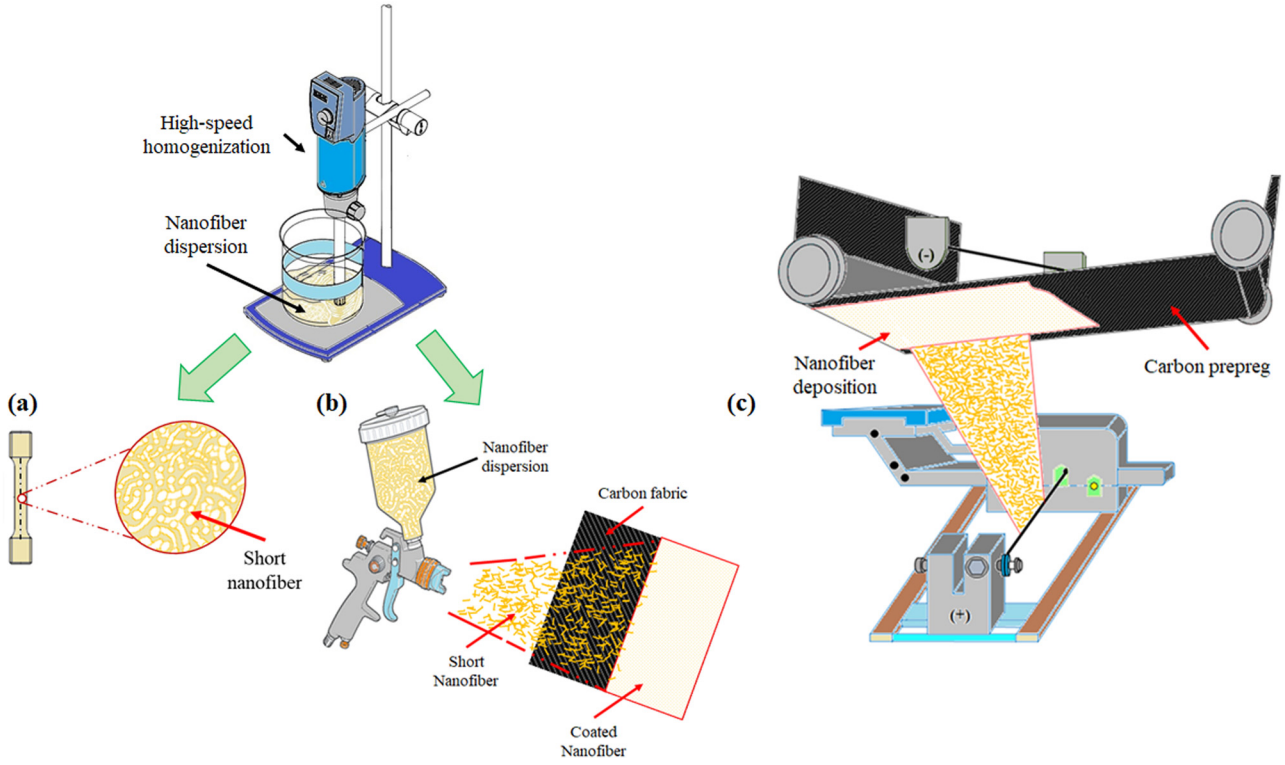

Figure 9: Short nanofiber application in (a) bulk matrix modification, (b) spray deposition, and (c) direct spinning.

fracture modes and mechanisms when they are incorporated at optimum concentration [117].

5.2 Spray deposition

A dispersion of short nanofibers, attained through sonication or mechanical cutting, can be used directly to alter interphase or interlaminar properties of fiber-reinforced nanocomposites (Figure 9(b)). A combination of suitable solvent and preparation technique has been highlighted to deposit short nanoparticle on fiber surface [118]. A major difference here, when compared to bulk matrix modification, is that solvent removal step is not required through advance equipment. As the purpose of solvent was to carry the nanofiber to fabric reinforcement surface, it can be allowed to evaporate at room temperature or in an oven, subsequently. Selection of solvent is crucial here as a volatile solvent will shorten evaporation time. Application of short nanofibers, using this technique, offers a window of tailoring interfaces to enhance interaction with matrices. Also, spray deposition is likely to improve the mechanical adhesion of nanofiber with micro-fiber reinforcement. Once the deposition is complete, lamina can be stacked to fabricate laminate using hot press or vacuum infusion.

5.3 Direct spinning

Another application area is to use prepreg as collector or substrate of nanofibers to enhance interlaminar fracture properties of fiber-reinforced nanocomposites [119]. This involves wrapping collecting drum with prepreg and spinning nanofibers (Figure 9(c)). Such an approach excludes the requirement of handling nanofiber veils for laminate fabrication since the lamina with deposited nanofibers will be stacked to cure resin through hot press. This approach has two major complications: (1) spinning time should not outlast prepreg cure time and (2) nanofiber melting temperature should be higher than curing temperature of prepreg.

More mechanical adhesion is possible since nanofibers are directly deposited on prepreg (Figure 10(a) and (b)). *In situ* short nanofiber techniques such as electric spark and entanglement loss are suitable for direct spinning. This is particularly so since short nanofiber cannot be collected from substrate, a feature that can restrict their applications.

This approach has been successfully utilized to improve mechanical properties of fiber-reinforced composites, primarily, that involves tensile [121,122], flexural [123–125], impact [126–129], indentation [130–132], interlaminar fracture toughness [133–135], fatigue [136,137], and viscoelastic [138] properties of laminated composites.

6 Discussion

A cursory glance at Table 4 provides an insight into the efficiency of diverse mechanisms adopted for short nanofiber preparation. Although, mechanical and ultrasonication-assisted cutting often show relation between processing time and nanofiber length (thus offering

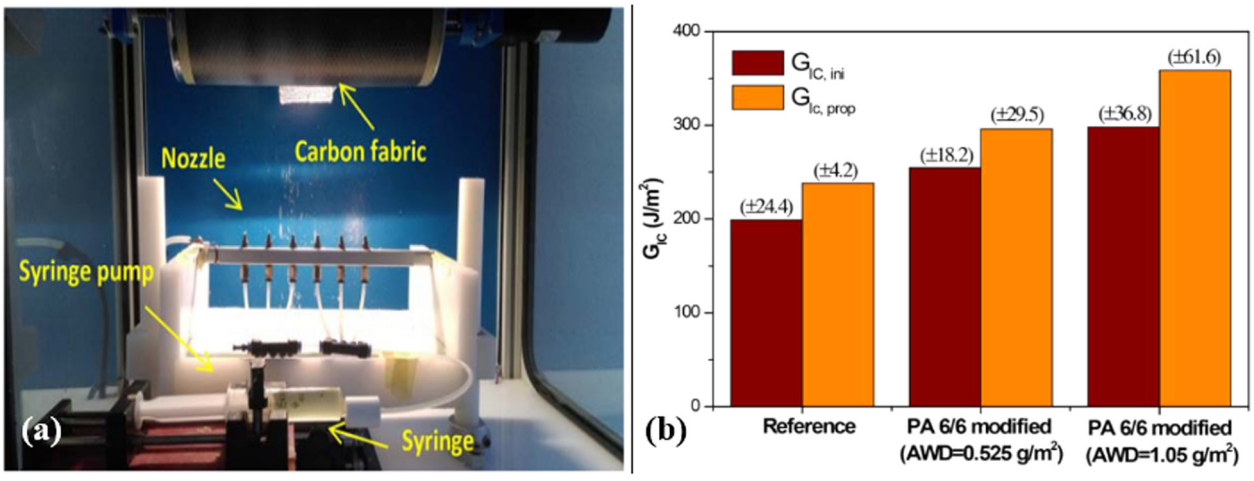

Figure 10: (a) Direct deposition of nanofibers on prepreg and (b) improvement in interlaminar fracture toughness [120]; Reproduced with permission from John Wiley and Sons.

Table 4: Summary of short nanofiber preparation parameters and results

Nanofiber	Diameter (nm)	Procedure	Nanofiber length (μm)	Aspect ratio	Ref.
Mechanical cutting					
PAN	300–400	Grinding (1 h), sonicating (10 min), and drying (60°C)	3–7	10–17.5	[52]
Poly (ST-*r*-VBP)	593	Mechanical homogenizing (1 h)	11 ± 17	18.54	[53]
P(MMA-*c*-VA)	1,000–3,000	Liquid nitrogen-assisted blade cutting	50–100	20–30	[55]
PEO/PLA copolymer	1,000–3,000	Liquid nitrogen-assisted blade cutting	5–15	5	[141]
PLA	300–1,300	Mechanical stirring (1,500 rpm for 24 h)	220 ± 112	169.2–733.3	[84]
PAA	320	Blender cutting at −18°C (3,500 rpm for 1 min)	87 ± 53	271.8	[82]
TiO_2/PVP	200	Mortar and pestle crushing	1–10	0.5–50	[92]
GO/Fe_2O_3/PAN	300	Homogenizing (16,000 rpm)	49.73	165.76	[59]
GLA/PVA	910	Homogenizing (13,000 rpm for 15 min)	27	29.67	[60]
PI	75	Blade cutting (3,500 rpm for 2 min)	14	186.66	[64]
PI	75	Blade cutting (3,500 rpm for 2 min)	20	1428.57	[57]
Poly(MA-*co*-MMA-*co*-MABP)	1,000	Blade cutting (5,000 rpm for 45 s)	150	150	[66]
PAN	1,100	Blade cutting (23,000 rpm for 10 min)	442 ± 171	401.81	[68]
CA/PCL	900	Blending (19,600 rpm for 10 min)	95.21	105.55	[71]
PAN/PI	453	Blending (19,600 rpm for 10 min)	123	271.52	[73]
Ultrasonication					
Silica	800	Sonication (15 min)	80	100	[102]
PLLA	771	UV irradiation (12 min) and sonication (amplitude 80%, run time 29 min)	5 ± 5	6.48	[24]
PLLA	244	Sonication (pulse on/off: 2 s/2 s)	39 ± 37	159.83	[105]
Titania	100	Sonication (1 h)	3	30	[104]
Electric spark					
Cellulose acetate	90–400	Power supply-assisted spark	100	250–1111.1	[106]
Entanglement loss					
Cellulose acetate	1,000	Finding critical concentration of entanglement loss	50–150	50–150	[39]
TiO_2/cellulose acetate	310–370	Optimum nanoparticle concentration	47	127–151	[107]
PMMA	50–3,000	Finding critical concentration of entanglement loss	1–1,000	20–333.3	[41]
Chemical treatment					
PLA	958, 325, and 152	Aminolysis under shearing force (500 rpm)	5.2–15.8	16.49–34.21	[23]

Note: Single value of length or diameter represent average taken. In case range of nanofiber diameter/length are given, aspect ratio is calculated by dividing smaller value of length with corresponding smaller value of diameter and identically for larger values.

length control), retrieved nanofiber yet have a wider length range (few to hundreds of microns). Additionally, these methods are found to be effective for rigid polymers as against ductile polymers. However, a combination of mechanical/ultrasonication technique with chemical/physical treatment has been found to be less time taking and offering higher yield. Entanglement loss is a viable approach but with a limitation on retrieval of nanofiber to be used as filler in nanocomposites. Chemical treatment exploits the phase structure of polymer that has negative consequences on fiber morphology. In addition to the mechanical and chemical methods mentioned above, ball milling has been reported to be used for PAN nanofiber breakage. However, it is severely limited in terms of offering control over the length of nanofibers [139] except in an isolated study where cryo-milling was effective in retrieving the short nanofibers (L = 27 μm) of itraconazole/hydroxypropyl methylcellulose. Also, selection of milling for brittle PAN nanofibers indicates its limitation to handle ductile nanofibers. This has been confirmed by utilizing cryo-milling for PS nanofibers, where it led to plastic deformation of nanofibers and flake-like morphology [24].

Nature of solvent–polymer interaction is critical, too, in nanofiber breakage using mechanical methods. For instance, water is unsuitable solvent to be used for

hydrophobic polymers as it facilitates nanofiber agglomeration. Solvent should be chosen to energetically favor fiber–solvent interaction over fiber–fiber interaction. Such a selection will help wet and infiltrate the non-woven thereby improving bubble cavitation and explosion inducing nanofiber breakage [105]. Another solution is nanofiber surface treatment to improve hydrophilic character, but the downsides are increment in diameter, altered morphology, or mechanical properties degradation.

Nanofiber geometrical parameters and configuration too affect the shortening phenomenon. Nanofibers has been, so far, collected in non-woven and aligned configurations. Whereas, non-woven configuration is attained by default, alignment is usually achieved by rotating the collecting drum at high speeds. Aligned nanofibers breakage was reported to be convenient with lower average fiber length and standard deviation compared to those of random nanofibers [24]. Two factors are considered influential here: density of nanofiber network and molecular chain alignments. In a non-woven and entangled web, infusion of solvent bubbles and implosion to flex nanofibers into breakage is difficult. This mechanism is likely to be much more efficient in aligned nanofiber with relatively uniform linear density of network. In addition to macroscopic alignment of nanofibers, a higher degree of molecular chain alignment is induced in nanofiber internal structure thereby improving strength and reducing elongation at break [140]. The latter property facilitates the breakage of nanofibers. Diameters of nanofiber has been reported to be a factor affecting the average nanofiber length in short nanofiber preparation. The higher the diameter, the higher will be the force required to fracture it. Hence, average nanofiber length and nanofiber diameter has linear relationship if all other variables are kept constant.

The effect of environmental parameters, especially temperature, was investigated to be significant in preparing short nanofibers. In general, relationship of nanofiber breakage with room temperature or higher is weak. However, a comparative study maintaining sub-zero (–80°C) temperature while sonication of nanofiber showed relation between sonication time and nanofiber length [105]. A general lesson is to keep the temperature below the glass transition temperature of polymer nanofiber.

Figure 11(a) shows comparison of nanofiber length distribution offered by several techniques. Most of the reported studies employed mechanical cutting, hence a wider data spectrum is obvious for this technique. Average lengths reported for mechanical cutting, sonication, entanglement loss, electric spark, and chemical treatment methods were in the range of 5–650, 5–39, 120–500, 100, and 10.5 µm, respectively. Identically, lowest aspect ratio, calculated from reported data, was plotted to assess efficacy of different techniques (Figure 10(b)). This range was 5–271.8, 6.48–159.83, 20–127, 250, and 16.9 for mechanical cutting, sonication, entanglement loss, electric spark, and chemical treatment methods, respectively.

7 Conclusion and perspective

Short nanofiber are attractive reinforcing fillers and materials for nanocomposites and scaffold fabrication,

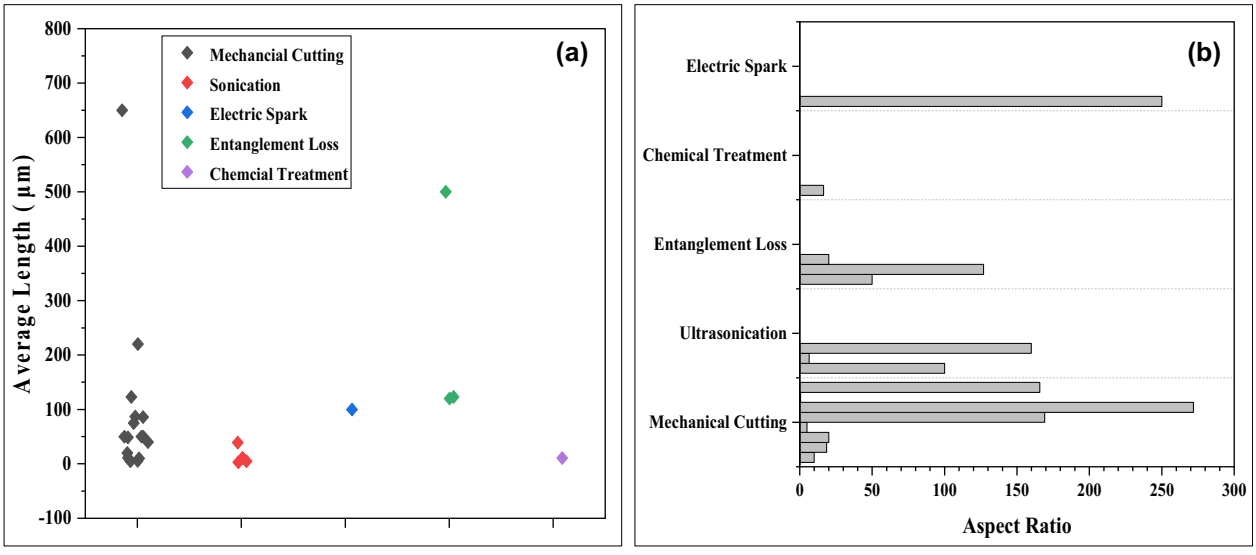

Figure 11: (a) Average length and (b) aspect ratio offered by diverse short nanofiber preparation techniques.

respectively. They are believed to impart diverse properties such as transparency and mechanical strength, simultaneously, in reinforced matrix. Control over aspect ratio with minimal deviation in nanofiber length is, therefore, an objective for material scientists and engineers. Attempts, so far, in this way offer some insights into scission of nanofiber. An aspect ratio in the range of 5–250 is invariably available using different techniques. In general, ductile polymers are hard to be fractured using mechanical- or sound energy-assisted breakage. Employed techniques induce pitting or roughening of nanofiber surface except entanglement loss and thermal fracture mechanisms. There is clear evidence that a combination of mechanisms (treatment and shear forces or UV etching and sonication) provides higher control over processing of short nanofiber.

A review of the literature reveals several gaps, in the domain of fabrication and measurements of nanofibers, that can help advance the understanding and applicability of short nanofibers. Some of these themes in the areas of nanofiber spinning, length measurements, and application are highlighted here.

1) Hydrophobicity of polymeric nanofibers have proved to be an impediment in solvent-assisted breakage of nanofibers. Core-shell configuration of nanofibers is a facile approach to simultaneously benefit from surface (shell) functionality and bulk (core) mechanical properties. Thin hydrophilic shell characteristics, obtained through controlling flow rate, can be combined with high mechanical bulk properties to facilitate nanofiber breakage together with matrix reinforcement. Also, this configuration offers a route to escape complications associated with chemical- or UV rays-assisted inducement of hydrophilic character.
2) Optimizing aspect ratio of nanofiber is critical to ascertain its effectiveness as reinforcement. This involves accurate determination of average nanofiber length in a liquid sample. So far, microscopic images have been reported to be facilitating nanofiber measurements. Hence, there is a need to correlate nanofiber geometrical parameters with conventional particle size analysis algorithms to get representative average length distributions. A related issue is of ensuring homogeneous dispersion of nanofiber sample. For that, turbidity measurements can be an indicator, indirectly, of dispersion level.
3) Solvent-assisted nanofiber breakage offers a facile option to mix the dispersion with resin for nanocomposite fabrication. However, techniques employing entanglement loss and electric spark mechanisms inherently limit short nanofiber application in composite reinforcement. For fiber-reinforced composites, short nanofibers can be collected directly on fabric/prepreg prior to fabrication. This will eliminate not only sample handling/processing step from fabrication stage but also help tailor interface properties of fiber-reinforced nanocomposites.

It is expected that future efforts, in this domain, not only will provide greater control over aspect ratio but help investigate the efficiency of these techniques for metallic and ceramic nanofibers in addition to polymeric ones. The opportunity to scale up the short nanofiber preparation and length measurement techniques will establish novel relationships between nanofiber geometrical parameters and nanocomposite performance.

Acknowledgements: First author would like to thank Higher Education Commission, Pakistan for providing financial assistance.

Funding information: This work was accomplished with monetary assistance provided by Universiti Teknologi Malaysia through grant number R.J130000.7351.4B553.

Author contributions: All authors have accepted responsibility for the entire content of this manuscript and approved its submission.

Conflict of interest: The authors state no conflict of interest.

References

[1] Wang G, Yu D, Kelkar AD, Zhang L. Electrospun nanofiber: Emerging reinforcing filler in polymer matrix composite materials. Prog Polym Sci. 2017;75:73–107.
[2] Canal C, Ginebra M. Fibre-reinforced calcium phosphate cements: a review. J Mech Behav Biomed Mater. 2011;4(8):1658–71.
[3] Paul DR, Robeson LM. Polymer nanotechnology: nanocomposites. Polymer. 2008;49(15):3187–204.
[4] Giannelis EP. Polymer layered silicate nanocomposites. Adv Mater. 1996;8(1):29–35.
[5] Fu SY, Lauke B, Mäder E, Hu X, Yue CY. Fracture resistance of short-glass-fiber-reinforced and short-carbon-fiber-reinforced polypropylene under Charpy impact load and its dependence on processing. J Mater Process Technol. 1999;89:501–7.
[6] Fu S-Y, Lauke B, Mäder E, Yue C-Y, Hu X. Tensile properties of short-glass-fiber-and short-carbon-fiber-reinforced polypropylene composites. Composites Part A Appl Sci Manuf. 2000;31(10):1117–25.
[7] Yao B, Wang G, Ye J, Li X. Corrosion inhibition of carbon steel by polyaniline nanofibers. Mater Lett. 2008;62(12–13):1775–8.

[8] Al-Saleh MH, Sundararaj U. Review of the mechanical properties of carbon nanofiber/polymer composites. Composites Part A Appl Sci Manuf. 2011;42(12):2126–42.
[9] Endo M, Kim YA, Hayashi T, Nishimura K, Matusita T, Miyashita K, et al. Vapor-grown carbon fibers (VGCFs): basic properties and their battery applications. Carbon. 2001;39(9):1287–97.
[10] Mahalingam S, Edirisinghe M. Forming of polymer nanofibers by a pressurised gyration process. Macromol Rapid Commun. 2013;34(14):1134–9.
[11] Gibson P, Schreuder-Gibson H, Rivin D. Transport properties of porous membranes based on electrospun nanofibers. Colloids Surf A Physicochem Eng Asp. 2001;187:469–81.
[12] Fuenmayor CA, Lemma SM, Mannino S, Mimmo T, Scampicchio M. Filtration of apple juice by nylon nanofibrous membranes. J Food Eng. 2014;122:110–6.
[13] Kumbar SG, James R, Nukavarapu SP, Laurencin CT. Electrospun nanofiber scaffolds: engineering soft tissues. Biomed Mater. 2008;3(3):034002.
[14] Liao S, Li B, Ma Z, Wei H, Chan C, Ramakrishna S. Biomimetic electrospun nanofibers for tissue regeneration. Biomed Mater. 2006;1(3):R45–53.
[15] Holmes B, Castro NJ, Zhang LG, Zussman E. Electrospun fibrous scaffolds for bone and cartilage tissue generation: recent progress and future developments. Tissue Eng Part B Rev. 2012;18(6):478–86.
[16] Lee S, Kay Obendorf S. Developing protective textile materials as barriers to liquid penetration using melt-electrospinning. J Appl Polym Sci. 2006;102(4):3430–7.
[17] Deitzel JM, Kleinmeyer J, Harris D, Beck Tan NC. The effect of processing variables on the morphology of electrospun nanofibers and textiles. Polymer. 2001;42(1):261–72.
[18] Andrady AL. Science and technology of polymer nanofibers. Hoboken, New Jersey, USA: John Wiley & Sons; 2008.
[19] Chen S, John JV, McCarthy A, Xie J. New forms of electrospun nanofiber materials for biomedical applications. J Mater Chem B. 2020;8(17):3733–46.
[20] Dziemidowicz K, Sang Q, Wu J, Zhang Z, Zhou F, Lagaron JM, et al. Electrospinning for healthcare: Recent advancements. J Mater Chem B. 2021;9(4):939–51.
[21] Ramakrishna S. An introduction to electrospinning and nanofibers. Singapore: World Scientific; 2005.
[22] Yokoyama Y, Hattori S, Yoshikawa C, Yasuda Y, Koyama H, Takato T, et al. Novel wet electrospinning system for fabrication of spongiform nanofiber 3-dimensional fabric. Mater Lett. 2009;63(9–10):754–6.
[23] Kim TG, Park TG. Biodegradable polymer nanocylinders fabricated by transverse fragmentation of electrospun nanofibers through aminolysis. Macromol Rapid Commun. 2008;29(14):1231–6.
[24] Sawawi M, Wang TY, Nisbet DR, Simon GP. Scission of electrospun polymer fibres by ultrasonication. Polymer. 2013;54(16):4237–52.
[25] Fu S, Lauke B. Analysis of mechanical properties of injection molded short glass fibre (SGF)/calcite/ABS composites. J Mater Sci Technol. 1997;13(5):389–400.
[26] Fu S-Y, Lauke B. Characterization of tensile behaviour of hybrid short glass fibre/calcite particle/ABS composites. Composites Part A Appl Sci Manuf. 1998;29(5–6):575–83.
[27] Joshi M, Maiti SN, Misra A, Mittal RK. Influence of fiber length, fiber orientation, and interfacial adhesion on poly (butylene terephthalate)/polyethylene alloys reinforced with short glass fibers. Polym Compos. 1994;15(5):349–58.
[28] Bijsterbosch H, Gaymans R. Polyamide 6 – long glass fiber injection moldings. Polym Compos. 1995;16(5):363–9.
[29] Mordkovich V. Carbon nanofibers: a new ultrahigh-strength material for chemical technology. Theor Found Chem Eng. 2003;37(5):429–38.
[30] Tibbetts G, Lake M, Strong K, Rice B. A review of the fabrication and properties of vapor-grown carbon nanofiber/polymer composites. Compos Sci Technol. 2007;67(7–8):1709–18.
[31] Howe JY, Tibbetts GG, Kwag C, Lake ML. Heat treating carbon nanofibers for optimal composite performance. J Mater Res. 2006;21(10):2646–52.
[32] Ibrahim HM, Klingner A. A review on electrospun polymeric nanofibers: Production parameters and potential applications. Polym Test. 2020;90:106647.
[33] Esfahani H, Jose R, Ramakrishna S. Electrospun ceramic nanofiber mats today: Synthesis, properties, and applications. Materials. 2017;10(11):1238.
[34] Khalil A, Singh Lalia B, Hashaikeh R, Khraisheh M. Electrospun metallic nanowires: Synthesis, characterization, and applications. J Appl Phys. 2013;114(17):12-1.
[35] Jun Z, Youling Y, Kehua W, Jian S, Sicong L. Surface modification of segmented poly (ether urethane) by grafting sulfo ammonium zwitterionic monomer to improve hemocompatibilities. Colloids Surf B Biointerfaces. 2003;28(1):1–9.
[36] Demir MM, Yilgor I, Yilgor E, Erman B. Electrospinning of polyurethane fibers. Polymer. 2002;43(11):3303–9.
[37] Zong X, Kim K, Fang D, Ran S, Hsiao BS, Chu B. Structure and process relationship of electrospun bioabsorbable nanofiber membranes. Polymer. 2002;43(16):4403–12.
[38] Fathona IW, Khairurrijal K, Yabuki A. One-step fabrication of short nanofibers by electrospinning: effect of needle size on nanofiber length. In Advanced materials research. Switzerland: Trans Tech Publications; 2014.
[39] Fathona IW, Yabuki A. A simple one-step fabrication of short polymer nanofibers via electrospinning. J Mater Sci. 2014;49(9):3519–28.
[40] Tungprapa S, Puangparn T, Weerasombut M, Jangchud I, Fakum P, Semongkhol S, et al. Electrospun cellulose acetate fibers: effect of solvent system on morphology and fiber diameter. Cellulose. 2007;14(6):563–75.
[41] Greenfeld I, Zussman E. Polymer entanglement loss in extensional flow: Evidence from electrospun short nanofibers. J Polym Sci Part B Polym Phys. 2013;51(18):1377–91.
[42] Zucchelli A, Focarete ML, Gualandi C, Ramakrishna S. Electrospun nanofibers for enhancing structural performance of composite materials. Polym Adv Technol. 2011;22(3):339–49.
[43] Chew SY, Hufnagel TC, Lim CT, Leong KW. Mechanical properties of single electrospun drug-encapsulated nanofibres. Nanotechnology. 2006;17(15):3880–91.
[44] Hwang KY, Kim SD, Kim YW, Yu WR. Mechanical characterization of nanofibers using a nanomanipulator and atomic force microscope cantilever in a scanning electron microscope. Polym Test. 2010;29(3):375–80.

[45] Bazbouz MB, Stylios GK. The tensile properties of electrospun nylon 6 single nanofibers. J Polym Sci Part B Polym Phys. 2010;48(15):1719–31.
[46] Lin Y, Clark DM, Yu X, Zhong Z, Liu K, Reneker DH. Mechanical properties of polymer nanofibers revealed by interaction with streams of air. Polymer. 2012;53(3):782–90.
[47] Wendorff JH, Agarwal S, Greiner A. Electrospinning: materials, processing, and applications. Weinheim, Germany: John Wiley & Sons; 2012.
[48] Jiang S, Duan G, Schöbel J, Agarwal S, Greiner A. Short electrospun polymeric nanofibers reinforced polyimide nanocomposites. Compos Sci Technol. 2013;88:57–61.
[49] Richard-Lacroix M, Pellerin C. Molecular orientation in electrospun fibers: from mats to single fibers. Macromolecules. 2013;46(24):9473–93.
[50] Xu H, Jiang S, Ding C, Zhu Y, Li J, Hou H. High strength and high breaking load of single electrospun polyimide microfiber from water soluble precursor. Mater Lett. 2017;201:82–4.
[51] Jiang S, Duan G, Chen L, Hu X, Hou H. Mechanical performance of aligned electrospun polyimide nanofiber belt at high temperature. Mater Lett. 2015;140:12–5.
[52] Xu W, Feng Y, Ding Y, Jiang S, Fang H, Hou H. Short electrospun carbon nanofiber reinforced polyimide composite with high dielectric permittivity. Mater Lett. 2015;161:431–4.
[53] Yoshikawa C, Zhang K, Zawadzak E, Kobayashi H. A novel shortened electrospun nanofiber modified with a 'concentrated' polymer brush. Sci Technol Adv Mater. 2011;12(1):015003.
[54] Huang CF, Yoshikawa C, Zhang K, Hattori S, Honda T, Zawadzak E, et al. Fabrication of shortened electrospun fibers with concentrated polymer brush toward biomaterial applications. In Advanced materials research. Trans Tech Publ.; 2011.
[55] Kriha O, Becker M, Lehmann M, Kriha D, Krieglstein J, Yosef M, et al. Connection of hippocampal neurons by magnetically controlled movement of short electrospun polymer fibers – a route to magnetic micromanipulators. Adv Mater. 2007;19(18):2483–5.
[56] Zhao X, Yang F, Wang Z, Ma P, Dong W, Hou H, et al. Mechanically strong and thermally insulating polyimide aerogels by homogeneity reinforcement of electrospun nanofibers. Compos Part B: Eng. 2020;182:107624.
[57] Cheong JY, Mafi M, Benker L, Zhu J, Mader M, Liang C, et al. Ultralight, structurally stable electrospun sponges with tailored hydrophilicity as a novel material platform. ACS Appl Mater Interfaces. 2020;12(15):18002–11.
[58] Deuber F, Adlhart C. From short electrospun nanofibers to ultralight aerogels with tunable pore structure. CHIMIA Int J Chem. 2017;71(4):236–40.
[59] Feng Z-Q, Shi C, Zhao B, Wang T. Magnetic electrospun short nanofibers wrapped graphene oxide as a promising biomaterial for guiding cellular behavior. Mater Sci Eng C. 2017;81:314–20.
[60] Li Y, Wang J, Qian D, Chen L, Mo X, Wang L, et al. Electrospun fibrous sponge via short fiber for mimicking 3D ECM. J Nanobiotechnology. 2021;19(1):1–15.
[61] Si Y, Fu Q, Wang X, Zhu J, Yu J, Sun G, et al. Superelastic and superhydrophobic nanofiber-assembled cellular aerogels for effective separation of oil/water emulsions. ACS Nano. 2015;9(4):3791–9.
[62] Si Y, Wang X, Yan C, Yang L, Yu J, Ding B. Ultralight biomass-derived carbonaceous nanofibrous aerogels with superelasticity and high pressure-sensitivity. Adv Mater. 2016;28(43):9512–8.
[63] Duan G, Koehn-Serrano M, Greiner A. Highly efficient reusable sponge-type catalyst carriers based on short electrospun fibers. Macromol Rapid Commun. 2017;38(3):1600511.
[64] Jiang S, Reich S, Uch B, Hu P, Agarwal S, Greiner A. Exploration of the electrical conductivity of double-network silver nanowires/polyimide porous low-density compressible sponges. ACS Appl Mater Interfaces. 2017;9(39):34286–93.
[65] Duan G, Jiang S, Jérôme V, Wendorff JH, Fathi A, Uhm J, et al. Ultralight, soft polymer sponges by self-assembly of short electrospun fibers in colloidal dispersions. Adv Funct Mater. 2015;25(19):2850–6.
[66] Duan G, Jiang S, Moss T, Agarwal S, Greiner A. Ultralight open cell polymer sponges with advanced properties by PPX CVD coating. Polym Chem. 2016;7(15):2759–64.
[67] Mader M, Jérôme V, Freitag R, Agarwal S, Greiner A. Ultraporous, compressible, wettable polylactide/polycaprolactone sponges for tissue engineering. Biomacromolecules. 2018;19(5):1663–73.
[68] Drummer M, Liang C, Kreger K, Rosenfeldt S, Greiner A, Schmidt HW. Stable mesoscale nonwovens of electrospun polyacrylonitrile and interpenetrating supramolecular 1, 3, 5-benzenetrisamide fibers as efficient carriers for gold nanoparticles. ACS Appl Mater Interfaces. 2021;13(29):34818–28.
[69] Liao X, Hu P, Agarwal S, Greiner A. Impact of the fiber length distribution on porous sponges originating from short electrospun fibers made from polymer Yarn. Macromol Mater Eng. 2020;305(2):1900629.
[70] Jiang S, Helfricht N, Papastavrou G, Greiner A, Agarwal S. Low-density self-assembled poly (*N*-isopropyl acrylamide) sponges with ultrahigh and extremely fast water uptake and release. Macromol Rapid Commun. 2018;39(8):1700838.
[71] Xu T, Liang Z, Ding B, Feng Q, Fong H. Polymer blend nanofibers containing polycaprolactone as biocompatible and biodegradable binding agent to fabricate electrospun three-dimensional scaffolds/structures. Polymer. 2018;151:299–306.
[72] Xu T, Ding Y, Wang Z, Zhao Y, Wu W, Fong H, et al. Three-dimensional and ultralight sponges with tunable conductivity assembled from electrospun nanofibers for a highly sensitive tactile pressure sensor. J Mater Chem C. 2017;5(39):10288–94.
[73] Xu T, Zheng F, Chen Z, Ding Y, Liang Z, Liu Y, et al. Halloysite nanotubes sponges with skeletons made of electrospun nanofibers as innovative dye adsorbent and catalyst support. Chem Eng J. 2019;360:280–8.
[74] Liang Z, Zhang H, Huang R, Xu T, Fong H. Superhydrophobic and elastic 3D conductive sponge made from electrospun nanofibers and reduced graphene oxide for sweatproof wearable tactile pressure sensor. Polymer. 2021;230:124025.
[75] Xu T, Li X, Liang Z, Amar VS, Huang R, Shende RV, et al. Carbon nanofibrous sponge made from hydrothermally generated biochar and electrospun polymer nanofibers. Adv Fiber Mate. 2020;2(2):74–84.
[76] Xu T, Wang Z, Ding Y, Xu W, Wu W, Zhu Z, et al. Ultralight electrospun cellulose sponge with super-high capacity on absorption of organic compounds. Carbohydr Polym. 2018;179:164–72.

[77] Zhu J, Jiang S, Hou H, Agarwal S, Greiner A. Low density, thermally stable, and intrinsic flame retardant poly (bis (benzimidazo) benzophenanthroline–dione) sponge. Macromol Mater Eng. 2018;303(4):1700615.
[78] Zhu J, Breu J, Hou H, Greiner A, Agarwal S. Gradient-structured nonflammable flexible polymer membranes. ACS Appl Mater interfaces. 2019;11(12):11876–83.
[79] Xu T, Yao Q, Miszuk JM, Sanyour HJ, Hong Z, Sun H, et al. Tailoring weight ratio of PCL/PLA in electrospun three-dimensional nanofibrous scaffolds and the effect on osteogenic differentiation of stem cells. Colloids Surf B Biointerfaces. 2018;171:31–9.
[80] Jiang S, Greiner A, Agarwal S. Short nylon-6 nanofiber reinforced transparent and high modulus thermoplastic polymeric composites. Compos Sci Technol. 2013;87:164–9.
[81] Jiang S, Hou H, Agarwal S, Greiner A. Polyimide nanofibers by "Green" electrospinning via aqueous solution for filtration applications. ACS Sustain Chem Eng. 2016;4(9):4797–804.
[82] Langner M, Greiner A. Wet-laid meets electrospinning: nonwovens for filtration applications from short electrospun polymer nanofiber dispersions. Macromol Rapid Commun. 2016;37(4):351–5.
[83] Boda SK, Wang H, John JV, Reinhardt RA, Xie J. Dual delivery of alendronate and E7-BMP-2 peptide via calcium chelation to mineralized nanofiber fragments for alveolar bone regeneration. ACS Biomater Sci Eng. 2020;6(4):2368–75.
[84] Zhang X, Geven MA, Grijpma DW, Gautrot JE, Peijs T. Polymer-polymer composites for the design of strong and tough degradable biomaterials. Mater Today Commun. 2016;8:53–63.
[85] Chen W, Ma J, Zhu L, Morsi Y, -Ei-Hamshary H, Al-Deyab SS, et al. Superelastic, superabsorbent and 3D nanofiber-assembled scaffold for tissue engineering. Colloids Surf B Biointerfaces. 2016;142:165–72.
[86] Chen W, Chen S, Morsi Y, El-Hamshary H, El-Newhy M, Fan C, et al. Superabsorbent 3D scaffold based on electrospun nanofibers for cartilage tissue engineering. ACS Appl Mater Interfaces. 2016;8(37):24415–25.
[87] Wang X, Liu M, Li H, Yin A, Xia C, Lou X, et al. MgO-incorporated porous nanofibrous scaffold promotes osteogenic differentiation of pre-osteoblasts. Mater Lett. 2021;299:130098.
[88] Ye K, Liu D, Kuang H, Cai J, Chen W, Sun B, et al. Three-dimensional electrospun nanofibrous scaffolds displaying bone morphogenetic protein-2-derived peptides for the promotion of osteogenic differentiation of stem cells and bone regeneration. J Colloid Interface Sci. 2019;534:625–36.
[89] Chen W, Sun B, Zhu T, Gao Q, Morsi Y, El-Hamshary H, et al. Groove fibers based porous scaffold for cartilage tissue engineering application. Mater Lett. 2017;192:44–7.
[90] Deuber F, Mousavi S, Federer L, Hofer M, Adlhart C. Exploration of ultralight nanofiber aerogels as particle filters: capacity and efficiency. ACS Appl Mater Interfaces. 2018;10(10):9069–76.
[91] Huang Y, Lai F, Zhang L, Lu H, Miao YE, Liu T. Elastic carbon aerogels reconstructed from electrospun nanofibers and graphene as three-dimensional networked matrix for efficient energy storage/conversion. Sci Rep. 2016;6(1):1–11.
[92] Deniz AE, Celebioglu A, Kayaci F, Uyar T. Electrospun polymeric nanofibrous composites containing TiO_2 short nanofibers. Mater Chem Phys. 2011;129(3):701–4.
[93] Yao Q, Cosme JG, Xu T, Miszuk JM, Picciani PH, Fong H, et al. Three dimensional electrospun PCL/PLA blend nanofibrous scaffolds with significantly improved stem cells osteogenic differentiation and cranial bone formation. Biomaterials. 2017;115:115–27.
[94] Miszuk JM, Xu T, Yao Q, Fang F, Childs JD, Hong Z, et al. Functionalization of PCL-3D electrospun nanofibrous scaffolds for improved BMP2-induced bone formation. Appl Mater Today. 2018;10:194–202.
[95] Si Y, Yu J, Tang X, Ge J, Ding B. Ultralight nanofibre-assembled cellular aerogels with superelasticity and multifunctionality. Nat Commun. 2014;5(1):1–9.
[96] Xu T, Miszuk JM, Zhao Y, Sun H, Fong H. Electrospun polycaprolactone 3D nanofibrous scaffold with interconnected and hierarchically structured pores for bone tissue engineering. Adv Healthc Mater. 2015;4(15):2238–46.
[97] Cheong JY, Benker L, Zhu J, Youn DY, Hou H, Agarwal S, et al. Generalized and feasible strategy to prepare ultra-porous, low density, compressible carbon nanoparticle sponges. Carbon. 2019;154:363–9.
[98] Mohseni M, Delavar F, Rezaei H. The piezoelectric gel-fiber-particle substrate containing short PVDF-chitosan-gelatin nanofibers and mesoporous silica nanoparticles with enhanced antibacterial activity as a potential of wound dressing applications. J Macromol Sci Part A. 2021;58(10):694–708.
[99] Suslick KS, Nyborg WL. Ultrasound: its chemical, physical and biological effects. New York, USA: VCH Publishers; 1990.
[100] Brenner MP, Hilgenfeldt S, Lohse D. Single-bubble sonoluminescence. Rev Mod Phys. 2002;74(2):425–84.
[101] Inam F, Reece MJ, Peijs T. Shortened carbon nanotubes and their influence on the electrical properties of polymer nanocomposites. J Composite Mater. 2012;46(11):1313–22.
[102] Liu Y, Sagi S, Chandrasekar R, Zhang L, Hedin NE, Fong H. Preparation and characterization of electrospun SiO_2 nanofibers. J Nanosci Nanotechnol. 2008;8(3):1528–36.
[103] Chen Q, Zhang L, Yoon MK, Wu XF, Arefin RH, Fong H. Preparation and evaluation of nano-epoxy composite resins containing electrospun glass nanofibers. J Appl Polym Sci. 2012;124(1):444–51.
[104] Wang X, Xi M, Zheng F, Ding B, Fong H, Zhu Z. Reduction of crack formation in TiO_2 mesoporous films prepared from binder-free nanoparticle pastes via incorporation of electrospun SiO_2 or TiO_2 nanofibers for dye-sensitized solar cells. Nano Energy. 2015;12:794–800.
[105] Mulky E, Yazgan G, Maniura-Weber K, Luginbuehl R, Fortunato G, Bühlmann-Popa AM. Fabrication of biopolymer-based staple electrospun fibres for nanocomposite applications by particle-assisted low temperature ultrasonication. Mater Sci Eng: C. 2014;45:277–86.
[106] Fathona IW, Yabuki A. One-step fabrication of short electrospun fibers using an electric spark. J Mater Process Technol. 2013;213(11):1894–9.
[107] Fathona IW, Yabuki A. Short electrospun composite nanofibers: Effects of nanoparticle concentration and

surface charge on fiber length. Curr Appl Phys. 2014;14(5):761–7.
[108] Tao J, Shivkumar S. Molecular weight dependent structural regimes during the electrospinning of PVA. Mater Lett. 2007;61(11–12):2325–8.
[109] Celebioglu A, Uyar T. Cyclodextrin short-nanofibers using sacrificial electrospun polymeric matrix for VOC removal. J Incl Phenom Macrocycl Chem. 2018;90(1):135–41.
[110] Stoiljkovic A, Agarwal S. Short electrospun fibers by UV cutting method. Macromol Mater Eng. 2008;293(11):895–9.
[111] Ramos A, Cameán I, García AB. Graphitization thermal treatment of carbon nanofibers. Carbon. 2013;59:2–32.
[112] Sand Jespersen T, Nygård J. Probing induced defects in individual carbon nanotubes using electrostatic force microscopy. Appl Phys A. 2007;88(2):309–13.
[113] Huang YY, Terentjev EM. Dispersion of carbon nanotubes: mixing, sonication, stabilization, and composite properties. Polymers. 2012;4(1):275–95.
[114] Rennhofer H, Zanghellini B. Dispersion state and damage of carbon nanotubes and carbon nanofibers by ultrasonic dispersion: a review. Nanomaterials. 2021;11(6):1469.
[115] Sancaktar E, Aussawasathien D. Nanocomposites of epoxy with electrospun carbon nanofibers: mechanical behavior. J Adhes. 2009;85(4–5):160–79.
[116] Deshpande TD, Singh Y, Patil S, Joshi YM, Sharma A. Adhesion strength and viscoelastic properties of polydimethylsiloxane (PDMS) based elastomeric nanocomposites with embedded electrospun nanofibers. Soft Matter. 2019;15(28):5739–47.
[117] Chen Q, Wu W, Zhao Y, Xi M, Xu T, Fong H. Nano-epoxy resins containing electrospun carbon nanofibers and the resulting hybrid multi-scale composites. Compos Part B: Eng. 2014;58:43–53.
[118] Ali A, Andriyana A, Hassan S, Ang BC. Fabrication and Thermo-Electro and Mechanical Properties Evaluation of Helical Multiwall Carbon Nanotube-Carbon Fiber/Epoxy Composite Laminates. Polymers. 2021;13(9):1437.
[119] van der Heijden S, Daelemans L, De Schoenmaker B, De Baere I, Rahier H, Van Paepegem W, et al. Interlaminar toughening of resin transfer moulded glass fibre epoxy laminates by polycaprolactone electrospun nanofibres. Com Sci Tech. 2014;104:66–73.
[120] Beylergil B, Tanoğlu M, Aktaş E. Enhancement of interlaminar fracture toughness of carbon fiber–epoxy composites using polyamide-6, 6 electrospun nanofibers. J Appl Polym Sci. 2017;134(35):45244.
[121] Bilge K, Venkataraman S, Menceloglu YZ, Papila M. Global and local nanofibrous interlayer toughened composites for higher in-plane strength. Compos Part A Appl Sci Manuf. 2014;58:73–6.
[122] Bilge K, Yorulmaz Y, Javanshour F, Ürkmez A, Yılmaz B, Şimşek E, et al. Synergistic role of *in situ* crosslinkable electrospun nanofiber/epoxy nanocomposite interlayers for superior laminated composites. Compos Sci Technol. 2017;151:310–6.
[123] Meng F, Zhao R, Zhan Y, Liu X. Design of thorn-like micro/nanofibers: fabrication and controlled morphology for engineered composite materials applications. J Mater Chem. 2011;21(41):16385–90.
[124] Herwan J, Al-Bahkali E, Khalil KA, Souli M. Load bearing enhancement of pin joined composite laminates using electrospun polyacrylonitrile nanofiber mats. Arab J Chem. 2016;9(2):262–8.
[125] Meng F, Zhan Y, Zhao R, Liu X. New strategy to reinforce and toughen composites via introducing thorns-like micro/nanofibers. Eur Polym J. 2012;48(1):74–8.
[126] Saghafi H, Fotouhi M, Minak G. Improvement of the impact properties of composite laminates by means of nano-modification of the matrix – A review. Appl Sci. 2018;8(12):2406.
[127] Özden-Yenigün E, Bilge K, Sünbüloğlu E, Bozdağ E, Papila M. High strain rate response of nanofiber interlayered structural composites. Composite Struct. 2017;168:47–55.
[128] Saghafi H, Minak G, Zucchelli A, Brugo TM, Heidary H. Comparing various toughening mechanisms occurred in nanomodified laminates under impact loading. Compos Part B Eng. 2019;174:106964.
[129] Zarei H, Brugo T, Belcari J, Bisadi H, Minak G, Zucchelli A. Low velocity impact damage assessment of GLARE fiber-metal laminates interleaved by Nylon 6, 6 nanofiber mats. Composite Struct. 2017;167:123–31.
[130] Goodarz M, Bahrami H, Sadighi M, Saber-Samandari S. Quasi-static indentation response of aramid fiber/epoxy composites containing nylon 66 electrospun nano-interlayers. J Ind Text. 2018;47(5):960–77.
[131] Goodarz M, Bahrami SH, Sadighi M, Saber-Samandari S. The influence of graphene reinforced electrospun nano-interlayers on quasi-static indentation behavior of fiber-reinforced epoxy composites. Fibers Polym. 2017;18(2):322–33.
[132] Zarei H, Nazari M, Koushali AG. Effect of interleaved composite nanofibrous mats on quasi-static and impact properties of composite plate. Iran Polym J. 2020;29(10):865–73.
[133] Ahmadloo E, Gharehaghaji AA, Latifi M, Mohammadi N, Saghafi H. How fracture toughness of epoxy-based nanocomposite is affected by PA66 electrospun nanofiber yarn. Eng Fract Mech. 2017;182:62–73.
[134] Li P, Liu D, Zhu B, Li B, Jia X, Wang L, et al. Synchronous effects of multiscale reinforced and toughened CFRP composites by MWNTs-EP/PSF hybrid nanofibers with preferred orientation. Compos Part A Appl Sci Manuf. 2015;68:72–80.
[135] Kelkar AD, Mohan R, Bolick R, Shendokar S. Effect of nanoparticles and nanofibers on Mode I fracture toughness of fiber glass reinforced polymeric matrix composites. Mater Sci Eng B. 2010;168(1–3):85–9.
[136] Daelemans L, van der Heijden S, De Baere I, Rahier H, Van Paepegem W, De Clerck K. Improved fatigue delamination behaviour of composite laminates with electrospun thermoplastic nanofibrous interleaves using the Central Cut-Ply method. Compos Part A: Appl Sci Manuf. 2017;94:10–20.
[137] Brugo T, Minak G, Zucchelli A, Yan XT, Belcari J, Saghafi H, et al. Study on Mode I fatigue behaviour of Nylon 6, 6 nanoreinforced CFRP laminates. Composite Struct. 2017;164:51–7.
[138] Ozden E, Menceloglu YZ, Papila M. Engineering chemistry of electrospun nanofibers and interfaces in nanocomposites for superior mechanical properties. ACS Appl Mater Interfaces. 2010;2(7):1788–93.
[139] Jo JH, Lee EJ, Shin DS, Kim HE, Kim HW, Koh YH, et al. *In vitro/in vivo* biocompatibility and mechanical properties of bioactive glass nanofiber and poly (ε-caprolactone)

composite materials. J Biomed Mater Res Part B Appl Biomater. 2009;91(1):213–20.
[140] Inai R, Kotaki M, Ramakrishna S. Structure and properties of electrospun PLLA single nanofibres. Nanotechnology. 2005;16(2):208–13.
[141] Thieme M, Agarwal S, Wendorff JH, Greiner A. Electrospinning and cutting of ultrafine bioerodible poly (lactide-*co*-ethylene oxide) tri- and multiblock copolymer fibers for inhalation applications. Polym Adv Technol. 2011;22(9):1335–44.